Mount Augustine: Exploring For A New Geothermal Resource In Southcentral Alaska

Guy Oliver[1], Moamen Gasser[2], Marcus Oesterberg[1], Anthony Pennino[3] and Paul Craig[3]

[1] Ignis Energy Inc., [2] Texas A&M University, [3] GeoAlaska Inc.

Keywords

Railbelt region, Renewable Energy Portfolio Standard, Mount Augustine, Stratovolcano, Upper Jurassic Naknek Formation, Resource Assessment, Monte Carlo Analysis, Power Density Potential, Volumetric Heat Recovery

Tuesday October 29th, 2024

Session 4E: Geology

King's 2 (Grand Ballroom)

6.10pm – 6.30pm

Mount Augustine: Exploring For A New Geothermal Resource In Southcentral Alaska

Guy Oliver[1], Moamen Gasser[2], Marcus Oesterberg[1], Anthony Pennino[3] and Paul Craig[3]

[1] Ignis Energy Inc., [2] Texas A&M University, [3] GeoAlaska Inc.

Keywords

Railbelt region, Renewable Energy Portfolio Standard, Mount Augustine, Stratovolcano, Upper Jurassic Naknek Formation, Resource Assessment, Monte Carlo Analysis, Power Density Potential, Volumetric Heat Recovery

ABSTRACT

Southcentral Alaska holds significant geothermal potential due to its location along the Pacific Ring of Fire, a region globally known for its volcanic activity and geothermal resources. The Cook Inlet Region lies above the Pacific Plate subduction zone and contains active volcanoes, including Mt. Augustine.

Alaska has some of the highest residential and commercial electricity prices in the nation, while its per capita energy consumption is the second highest, in part because of the State's small population, cold climate, and energy-intensive industries. Southcentral Alaska houses approximately 550,000 people (75% of the entire Alaskan population). Power sales in 2020 exceeded 4,408 GWh, of which 82% came from fossil-fuel produced electricity (natural gas and coal) and 18% from renewables (primarily hydroelectric). In December 2021, the Governor of Alaska requested a study on the potential impacts of achieving an 80% renewable energy portfolio for Southcentral Alaska.

Mt. Augustine is an andesitic stratovolcano typical of subduction zones and located in the Kamishak Bay in the southern part of the Cook Inlet, approximately 60 miles west of Anchor Point and 175 miles SW of Anchorage. Numerous previous researchers have concluded that it contains a shallow magma chamber making it attractive for geothermal exploitation. In September 2022, GeoAlaska was awarded a permit to explore for geothermal resources across 3 onshore tracts of land, totaling 3,048 acres on the southern part of Augustine Island, primarily where the Upper Jurassic Naknek Formation outcrops.

In the summer of 2023, Acoustic Magnetotelluric (AMT) data from 28 sites and gravity data from a further 215 locations were acquired, processed, and interpreted. Additionally, 20 rock samples

were collected from cliff sections along the southern margin of the island, primarily from within the outcropping Naknek Formation.

The jointly inverted geophysical data reveal an area in the southern part of the island of low resistivity and high density strata lying above a zone of higher resistivity. We interpret this as the sub-crop of the Naknek Formation acting as a seal, trapping a potential hydrothermal system below, within the fractured basement. The Naknek Formation is likely to underly much of the southern part of the island and is such an effective seal, it has all but limited any above sea-level surface geothermal features that one would expect for a typical andesitic geothermal resource. As such, we describe this Mt Augustine resource as being an atypical blind geothermal system, suggesting a largely horizontal circulation pattern. An analogue for this system could be Cerro Pabellón GPP in northern Chile, which has a current installed capacity of approximately 83 MWe.

As a result of this collected data, additional exploration activity will be undertaken during 2024/25 including the drilling of an exploration well.

1. Introduction and Context

GeoAlaska LLC was founded in 2020 with a desire to identify and exploit geothermal opportunities in Alaska, and to provide baseload carbon-free electricity for the benefit of the Alaskan people. In March 2023 Ignis Energy Inc, a sister company to Geolog International B.V., partnered with GeoAlaska in order to provide technical and project management support. Since 2021, GeoAlaska has created a geothermal exploration position that includes 2 prospective locations on State owned land and close to the Alaskan South Central Rail Belt Region, including 10,830 acres on the southern flank of Augustine Island (geothermal prospecting permits ADL 394080 and ADL 394374) and 6,376 acres on the southern/central flank of Mt. Spurr (geothermal resource leases 394178, 394179 and 394180). This paper focuses on exploring the geothermal potential at Augustine Island.

Southcentral Alaska holds significant potential due to its proximity to the Pacific Ring of Fire, a region globally known for its volcanic activity and geothermal resources (U.S. Energy Information Association, 2022). The Cook Inlet basin is a NW-SE trending forearc basin lying above the Aleutian subduction zone of southern Alaska (Haeussler, *et al*., 2000) which contains active volcanoes, including Mt. Augustine.

Alaska's electricity market has been growing rapidly, with a strong recent emphasis on renewable energy. In late May 2024, House Bill 50 was passed by House Alaskan lawmakers which included more favorable conditions to encourage geothermal prospecting in the State. There are no geothermal power plants operating in the State with an installed capacity greater than 0.5 MW.[1]

Alaska's per capita energy consumption is the second highest in the nation (U.S. Energy Information Association, 2024) in part because of the State's small population, cold climate and energy-intensive industries. Alaska also has some of the highest residential and commercial

[1] The Chena power plant located at Chena Hot Springs near Fairbanks has been in operation since 2006 and has an installed capacity of 0.4MW (Erkan *et al.*, 2008).

electricity prices in the nation (U.S. Energy Information Association, 2024). Finally, 70% of the Alaskan population lies within Southcentral Alaska's 'Railbelt region' (Asmus *et al.*, 2023).

The 'Railbelt region' refers to the interconnected electric grid that stretches approximately 700 miles from the city of Fairbanks in the north through Anchorage to the Kenai Peninsula in the south. About 75% of Alaska's population (approximately 550,000 residents) are served by the Railbelt region. As the largest electrical grid in the State, it is vital for statewide economic and community development. Based on 2020 usage, power sales were calculated to top 4,408 GWh, of which 82% came from fossil-fuel-produced electricity (primarily natural gas and coal) and 18% from renewables (primarily hydroelectric, Dahlstrom *et al.*, 2023). In 2022, the State passed and signed legislation through the Renewable Energy Portfolio Standard (RPS) that will allow Alaska to join 30 other States and 2 Territories in creating a renewable portfolio standard, that can be applied to the Railbelt region. A key element of the Governor's RPS is a firm commitment to transitioning to 30% sustainable power by 2030 and 80% by 2040 (Dahlstrom *et al.*, 2023).

There are concerns in the Cook Inlet region over the reliability of long-term natural gas supplies, with natural gas-fired power plants currently providing the bulk of electrical production in the region. Imported LNG may become necessary in the near future, would almost certainly lead to a higher price of electricity to the consumer (ENSTAR, 2024). In a recent 2023 survey conducted by the Alaska Center for Energy and Power (ACEP) 82% of 275 respondents 'somewhat' or 'strongly' favored geothermal technology as a future carbon neutral solution for the Railbelt region (Asmus, *et al*., 2023).

Geothermal power produced at Augustine Island could replace the current coal-fired power plants operating in the interior of Alaska and within the Railbelt region. These coal fired power plants produce a total of 816,000 MWh over a typical 12 month period, emitting a total of 1.7m tonnes of CO2e per year (Goodfellow and Birnbaum, 2023).

2. Geological Setting of Augustine Island

Augustine Island (otherwise referred to as Augustine Volcano or Mt. Augustine) is located in the southwestern Cook Inlet, Southcentral Alaska, approximately 175 miles southwest of Anchorage and 60 miles west of Anchor Point on the Kenai Peninsula (Figure 1).

Augustine Volcano, an andesitic stratovolcano began erupting before the late Wisconsin glaciation, some 75,000 years ago (Waitt and Begét, 2009) although Waythomas and Waitt, 1998 place the timing of the initial volcanic intrusion at approximately 40,000 years ago, on a small island of upper Jurassic Naknek Formation to upper Cretaceous sedimentary rock, in the Cook Inlet, Alaska (Waitt and Begét, 2009). Augustine Volcano most recently erupted in 2006 and prior to that, during the late 20th Century (Kamata et al., 1991, Power et al., 2006, Swanson and Kienle, 1988 and Waitt and Begét, 2009).

Several have postulated that Augustine volcano contains a relatively shallow magma chamber (Koulakov *et al.*, 2023, Eichelberger *et al.*, 2023, Power, 2023 (*pers comm)*) and we concur. Koulakov *et al.*, 2023 used arrival time data from local seismicity recorded by a number of seismic stations on the island to identify a shallow rigid core composed of igneous rocks but strongly fractured and saturated with fluids and melts. Above this the authors note a zone associated with degassing of deep fluids. We explore this further. Eichelberger *et al.*, 2023 and Power, 2023 (*pers*

comm) have postulated that the Augustine Volcano magma chamber is estimated to be at a depth of only 4 km with an expected temperature of 840°C and a de-gassing zone of approximately 300°C at around 1 km below sea level.

2.1 The southern flank of Augustine Island

Outcropping on the southern flank of Augustine Volcano are a approximately 500ft thick series of approximately 1 mile^2 gently dipping sedimentary rocks attributed to the Upper Jurassic Naknek Formation (Figure 2, Detterman and Reed, 1964, Detterman and Jones, 1974, Buffler, 1976, amongst others).

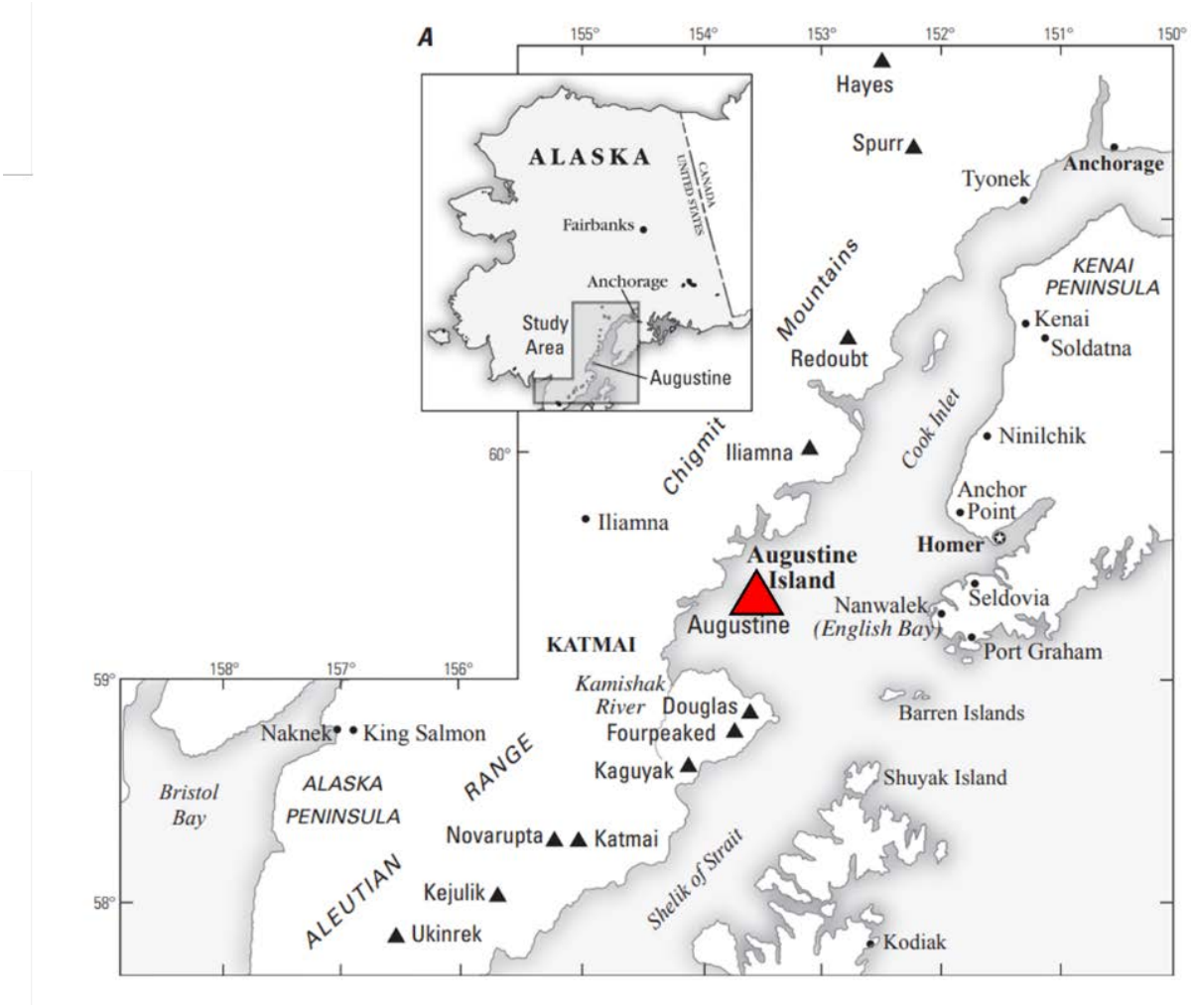

Figure 1: Cook Inlet area, Alaska; volcanoes shown as triangles, towns/cities as dots. Augustine Volcano shown as red triangle (modified from Waitt and Begét, 2009).

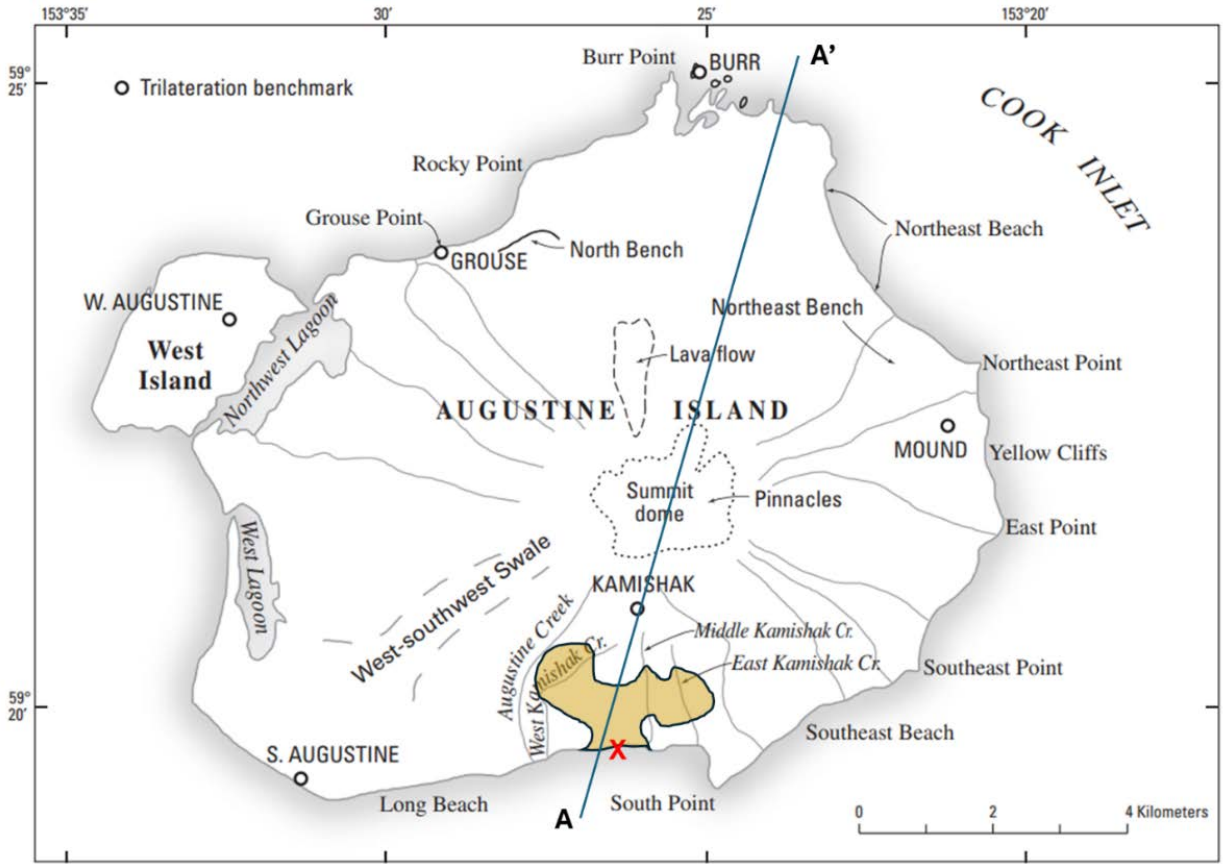

Figure 2: Approximate outcrop of Upper Jurassic Naknek Formation (brown shading) on the southern flank of Augustine Island (modified from Waitt and Begét, 2009). The red 'X' marks the location of the outcrop sampling (see below).

On Augustine Island, the Naknek Formation comprises a lower member of thin-bedded dark-gray siltstone to very fine sandstone and an upper member of thickly bedded medium to fine grained sandstone in places showing evidence of trough cross-bedding, lignite clasts and petrified wood (Waitt and Begét, 2009). The Naknek Formation on Augustine Island suggests deposition in a shallow restricted nearshore bay environment (Waitt and Begét, 2009). Interestingly, approximately 80 miles further north at Chisik Island, the Naknek Formation consists of deep-water channel deposits in sub-marine canyons (Herriott, T., *et al.*, 2016). Other workers (*e.g.* Koulakov *et al*., 2023b and Syracuse *et al.,* 2011) have reported that the uplifted Jurassic section is commonly zeolitized.

2.1.1 Outcrop sampling

During the Fall of 2023, GeoAlaska sub-sampled various sedimentary strata exposed in the beach and cliff section at the eastern extent of Long Beach (see Figure 2 for location). In total, 15 samples were collected of which 13 are of a sedimentary origin and 11 likely representative of different facies within the Naknek Formation (Figure 3 and Table 1). These sedimentary samples ranged from well cemented siltstone containing calcite cemented fractures to well cemented medium to coarse grained oxidized sandstones. Abundant bivalves were identified in some of the samples. XRD and XRF data from these outcrop samples indicate a clay mineralogy indicative of

chlorite and smectite (up to 29% in sample 20) with minor illite, throughout. In addition, in samples 13, 19 and 21 zeolites were identified ranging from 7.6 weight% (sample 21, Clinoptilolite) to 17.9 weight% (sample 13, Laumontite). Sample 19 was found to contain 10.7 weight% Heulandite.

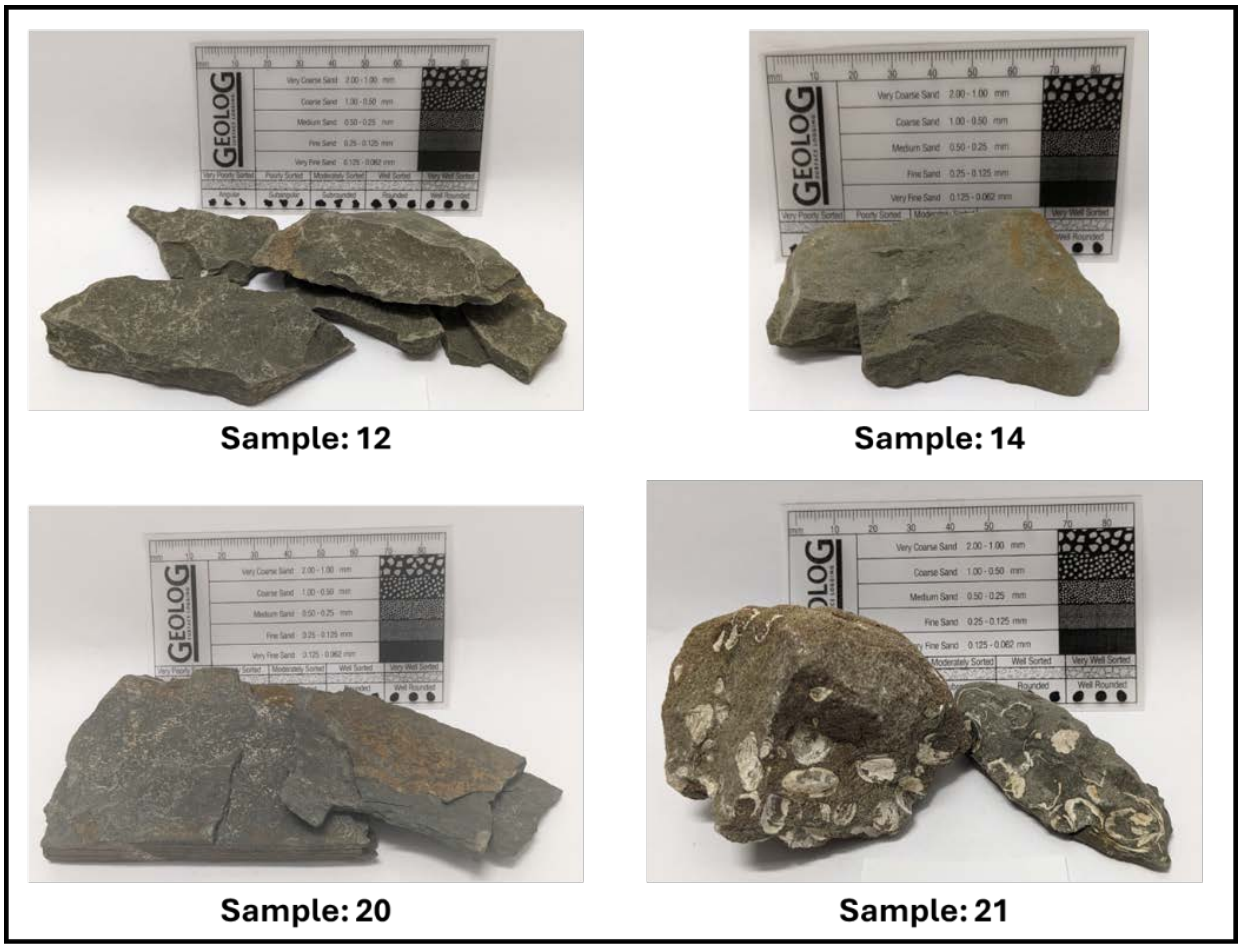

Figure 3: Outcrop samples from Long Beach, south Augustine Island. See Figure 2 for location of sampling.

2.1.2 Cross section

In their 2009 publication, Waitt and Begét include a NNE/SSW cross section of Augustine Island (see Figure 1 for cross section line) the southern portion of which is displayed in Figure 4 below. Note their assumptions of the Jurassic sub-crop, which this paper will explore further based on new MT, gravity and seismic data. It is the location, extent and composition of this Jurassic sub-crop that is a key component of the geothermal resource potential of the southern flank of Augustine Island.

3. Available Database

Table 2 summarizes the available data utilized for the exploration campaign to-date. In addition to the outcrop samples collected during the Fall of 2023, an initial Acoustic Magnetotelluric

(AMT) and Gravity survey was commissioned by GeoAlaska during the summer season of 2023 covering the entire ADL 394080 permit area. The MT survey consisted of 28 MT stations (Figure 5A) while the Gravity survey consisted of 215 stations (Figure 5B).

Table 1: Outcrop samples from Long Beach, south Augustine Island, sedimentological description. Highlighted rows refer to samples displayed in Figure 3.

Sample	Lithology	Colour	Density (g/cm^3)	Notes	Interpretation
1	Porfyric lava	Medium Grey (N5)	2.33	Hard, visible femic minerals (and some Obsidian), plagioclases and feldspars in a greyish groundmass.	Probable volcanic deposits
4	Porfyric lava	Grayish Red (10R 4/2)	2.52	Hard, millimeter sized feldspars and reddish femic crystals in a reddish groundmass.	
2	Claystone	Moderate Yellowish Brown (10YR 5/4)	1.94	Loose clay.	Probable recent Pleistocene to Late Holocene deposits
3	Claystone	Moderate Brown (5YR 4/4)	1.86	Soft claystone with some volcanic and sedimentary grains	
10	Sandstone	Dark Grey (N3)	2.42	Medium hard layered sandstone with cleavage. Presence of black fossils.	Probable Upper Jurassic sandstone and shale Naknek Formation
11	Sandstone	Olive Grey (5Y 4/1)	2.37	Hard coarse sandstone, reddish oxidation on some sides of the rock sample.	
12	Sandstone	Dark Grey (N3)	2.30	Hard fine grained sandstone. Presence of thin veins.	
13	Sandstone	Olive Grey (5Y 4/1)	2.33	Poorly well cemented coarse grained sandstone. Presence of fine-grained layers. Presence of dark micas.	
14	Sandstone	Olive Black (5Y 2/1)	2.15	Moderately hard. Presence of localized oxidation.	
15	Sandstone	Olive Black (5Y 2/1)	2.30	Hard fine grained layered sandstone. Presence of veins.	
17	Calcite veins in sandstone	Dark Grey (N3)	2.42	Pseudo-acicular/prysmatic veins witihn a fine grained sandstone. Calcite veins are coated by iron oxides.	
18	Siltstone	Dark Grey (N3)	2.52	Very hard cemented siltstone. presence of veins (calcite?).	
19	Sandstone	Olive Grey (5Y 4/1)	2.24	Moderately hard coarse grained sandstone. Slightly layered.	
20	Siltstone/Sandstone	Dark Grey (N3)	2.25	Moderately hard laminated coarse grained siltstone/fine grained sandstone . Slightly cemented.	
21	a) CG Sandstone; b) FG Sandstone	a) Light Olive Grey (5Y 5/2); b) Dark	2.42	a) Moderately hard, cemented, abundant fossils (bivalves) ; b) Hard, presence of fossils (bivalves) and veins.	

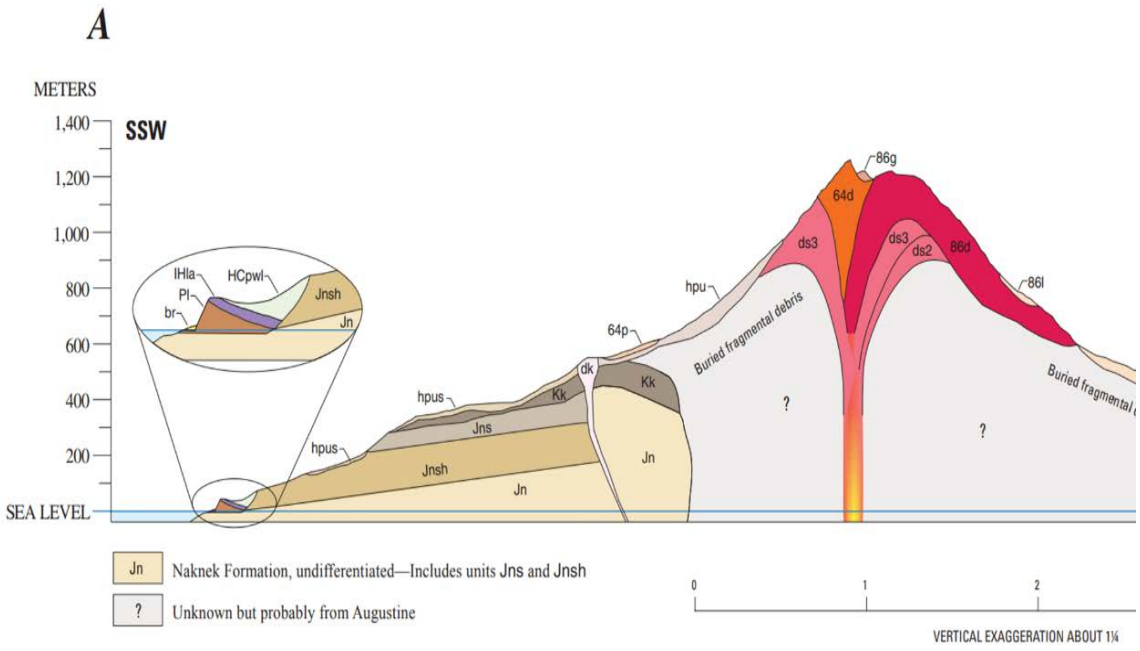

Figure 4: Cross section of the southern flank of Augustine Island (after Waitt and Begét, 2009).

Table 2: Summary of the available data utilized to-date for the exploration campaign on Mt. Augustine.

Data Type	Raw Data	Output Data	Interpreted Data	Notes	Reference
Geologic Structure	Yes	Yes	Yes	-	(Waitt and Begét, 2009) (Syracuse et al., 2011) (Koulakov et al., 2023b) Field studies, 2023
Temperature Logs for Shallow Wells	No	No	No	-	-
MT Data	Yes	Yes	Yes	AMT not MT.	Field studies, 2023
Resistivity Survey	Yes	Yes	Yes	With AMT Data above.	Field studies, 2023
Seismic Survey	Yes	Yes	Yes	The data is given in DAT file by (Koulakov et al., 2023b). The raw provided by USGS	(Syracuse et al., 2011) (Koulakov et al., 2023b)
Water Chemistry	Yes	Yes	Yes	Summit fumarole gas measurements from 2008 (5) & 2010 (3)	(Evans et al., 2015)
Gravity Data	Yes	Yes	Yes	In conjunction with AMT survey	Field studies 2023
Eruptions	Yes	Yes	Yes		(Kamata et al., 1991; Power et al., 2006; Swanson and Kienle, 1988)

In addition, GeoAlaska used catalog data provided by the Alaska Volcano Observatory (AVO) which includes arrival times of seismic *P* and *S* waves recorded by permanent seismic networks operating on the volcano. In this study we used data from January 2001 to December 2017, which included 6624 events recorded by 15 permanent stations deployed on the flanks of the volcano.

4. Geophysical Data Interpretation and Modelling

4.1 AMT and Gravity Data

From the AMT and Gravity data, a combined 3D inversion model was built using Geotools and RLM-3D code. The resulting 3D resistivity and density volumes were uploaded into Leapfrog Energy software where depth and vertical slices were extracted to visualize any low-resistivity and high-density anomalies. The visualizations were complemented by uploading the geological map of Mt. Augustine including the location of any potential geothermal elements.

The generated model revealed a sector with a convergence of low resistivity and high-density volumes on the southern flank of Augustine Volcano that could represent a working hydrothermal system, underlying a geothermal clay cap.

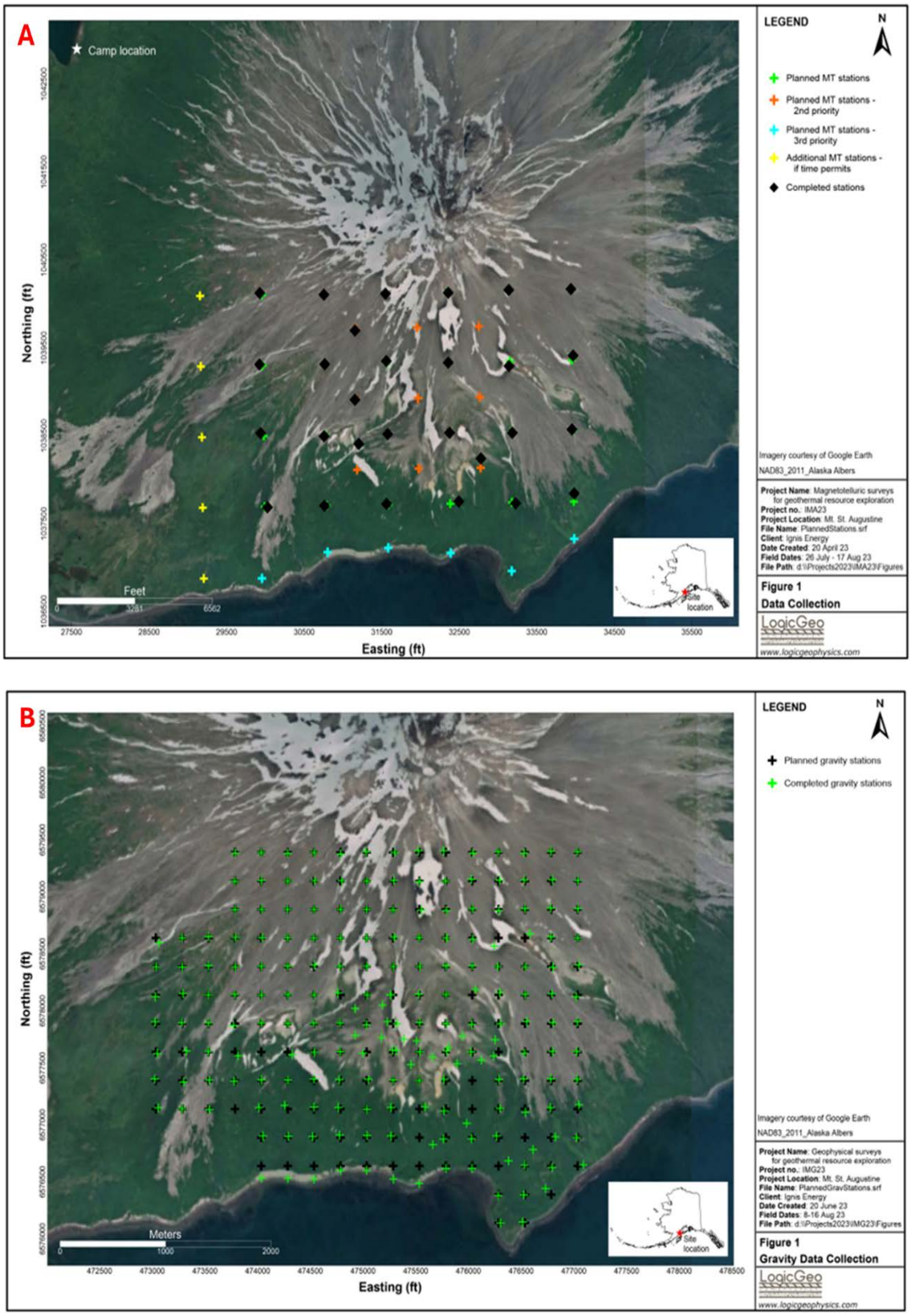

Figure 5: Maps showing the location and number of collected data from AMT (A) and Gravity (B)

4.2 Seismic Data

LOTOS code has been used for the seismic inversion and to construct the 3D visualization of Mt Augustine seismic data (Koulakov, 2009). The *P* and *S* wave velocities have been analyzed to get an insight on the potential geothermal reservoir tomography. The limitation and details of the code are beyond the scope of this article so the reader is referred to Koulakov, (2009); Koulakov et al., (2023b); Koulakov, (2020) for more information. The 3D inversion was sliced into 4 vertical cross-sections Figure 6) and 5 horizontal cross-sections. The data filtration was based on the approach of Koulakov, *et al.* 2023 which resulted in a total of 3,127 events with 10,680 P-wave picks and 11,080 S-wave picks. Although our approach is similar to Koulakov *et al.* (2023), their main focus was the volcanic pluming system, while our main focus is identifying a potential geothermal resource. Figure 7 shows the absolute P (V_P) and S (V_S) waves velocities for vertical and horizontal cross-sections. Also, the anomalies in P (dV_P) and S (dV_S) wave velocities are presented in Figure 8. The relatively similar count for P-wave picks and S-wave picks made it easier to obtain the ratio of dV_P/dV_S (shown in Figure 8). It is noted that in each of the cross-sections displayed in Figures 7 and 8, the lack of seismic events away from the central region is due to a limited number of seismic stations over the flanks of the volcano.

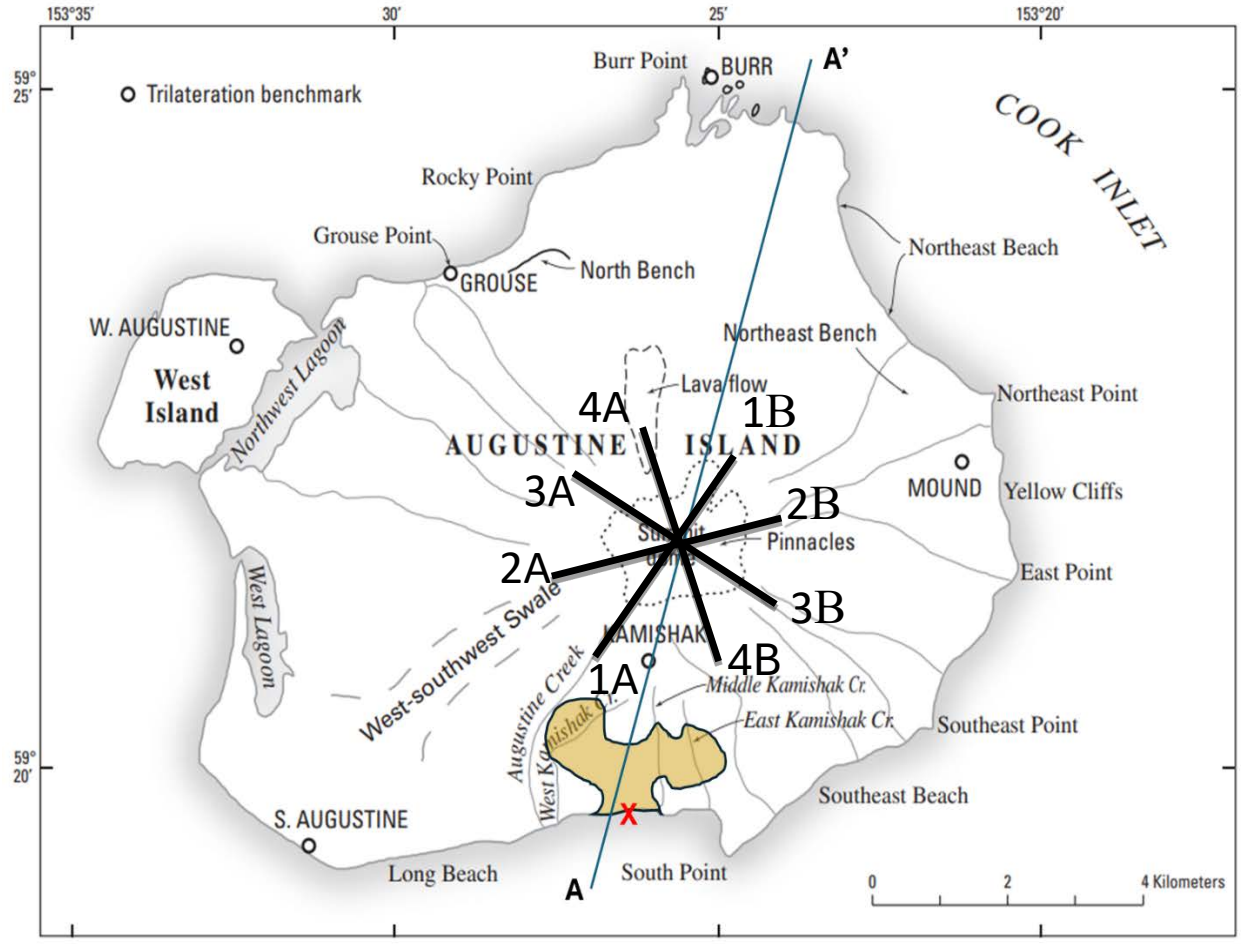

Figure 6: Locations of the 4 vertical seismic sections across Mt Augustine. Sections 1A-1B and 4A-4B are most relevant to this paper and will be discussed further.

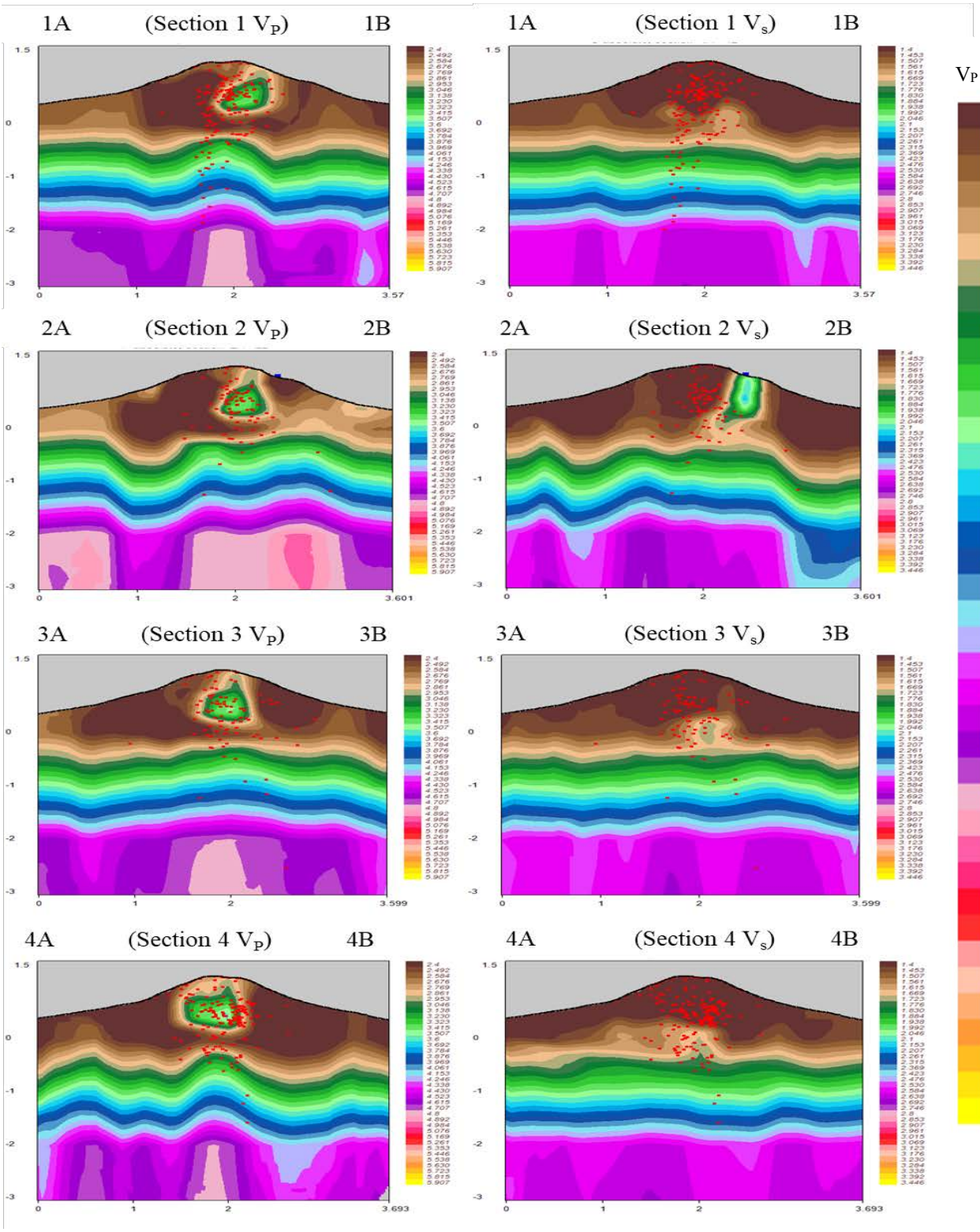

Figure 7: V_P (left column) and V_S (right column) measured in Km/sec for the 4 vertical sections (1 to 4) shown in Figure 6. The red dots represent measured seismic events, Y-axis is the elevation/depth above/under sea-level in Km and X-axis is horizontal displacement in Km along the 4 vertical seismic sections (shown in Figure 6) starting from 0 at point A and ending at point B in all subfigures.

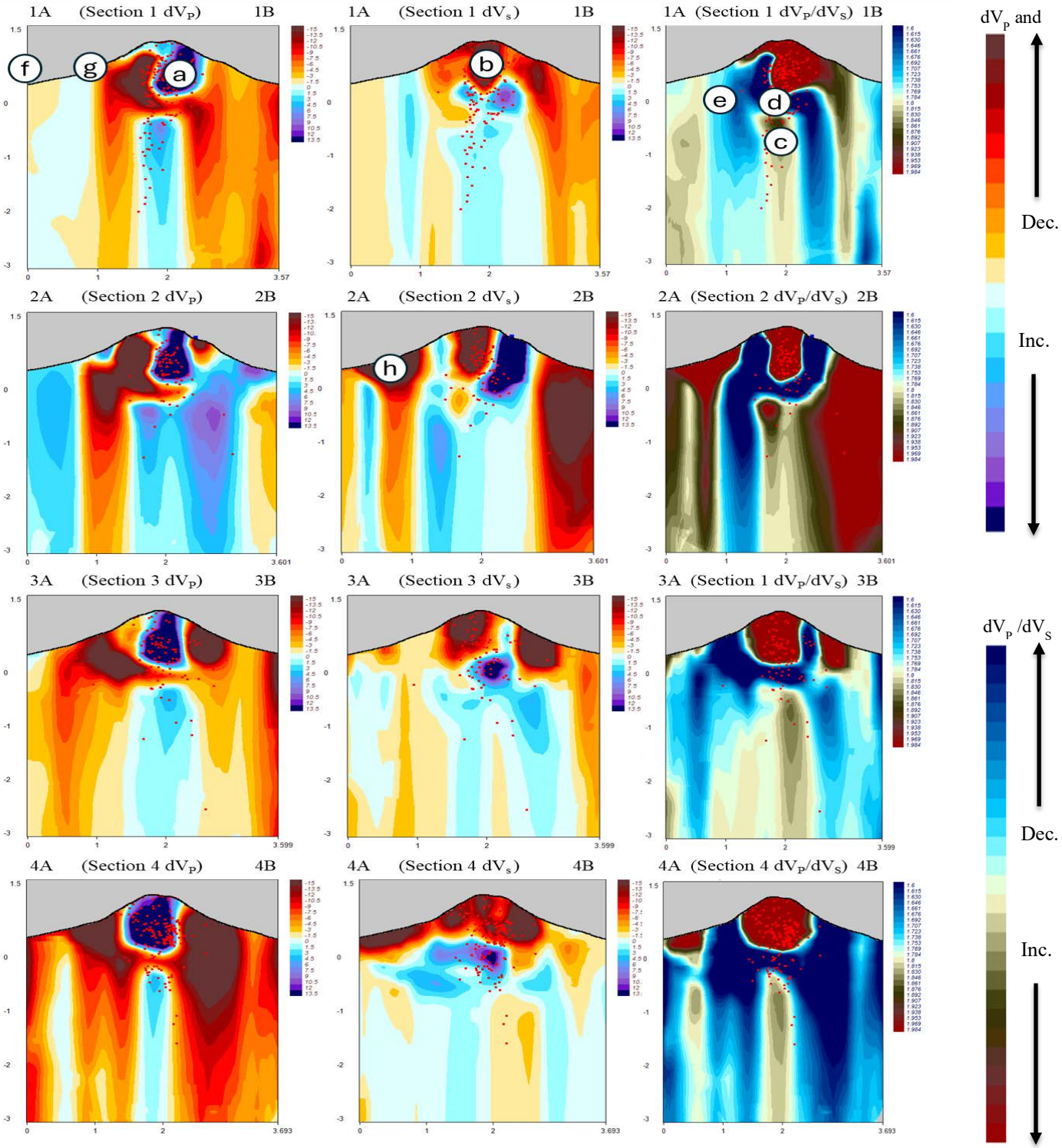

Figure 8: Shows dV_P (%) in the left column, dV_S (%) in the middle column and dV_P/dV_S (dimensionless) in the right column for the 4 vertical sections (1 to 4) shown in Figure 6. The red dots, Y-axis and X-axis are the same as described in Figure 7. See text for explanation of annotations a through h.

5. Subsurface Modelling

5.1 Geological Model (incorporating the AMT and Gravity data)

Figure 9 below is adapted from Waitt and Begét, 2009 and illustrates the geological model of the potential geothermal resource below the southern flank of Augustine Volcano. Outcrop data suggests that the Upper Jurassic sedimentary pile (light brown color on Figure 9, and acronyms Jnsh and Jns) has been faulted due to compression, probably as a result of the initial volcanic intrusion. These faults are likely to have been clay smeared reducing their effectiveness to form conduits to vertical fluid flow. It is more likely that any downward meteoric fluid flow occurs through or at the contact between the more porous volcanic sediments that onlap the Jurassic sub-crop.

XRD data from outcrop samples reveals that the Jurassic sediments can contain up to 29% smectite. In the sub-surface where there is interaction between super-heated brines and the sedimentary rock (yellow surfaces in Figure 9) this percentage volume is likely to be more and thus the Jurassic sub-crop is predicted to form an excellent seal or clay cap to any underlying hydrothermal system contained within the fractured basement (pink polygons in Figure 9). In fact, we believe the Jurassic sub-crop is such a good seal, it is preventing any upward movement of hydrothermal fluids, resulting in a more horizontal circulation pattern for the trapped hydrothermal fluids (Figure 9). A working hypothesis is that hydrothermal fluids could be reaching the surface on the sub-sea lower flanks of Augustine Island, although as of yet, there is no direct evidence to corroborate this.

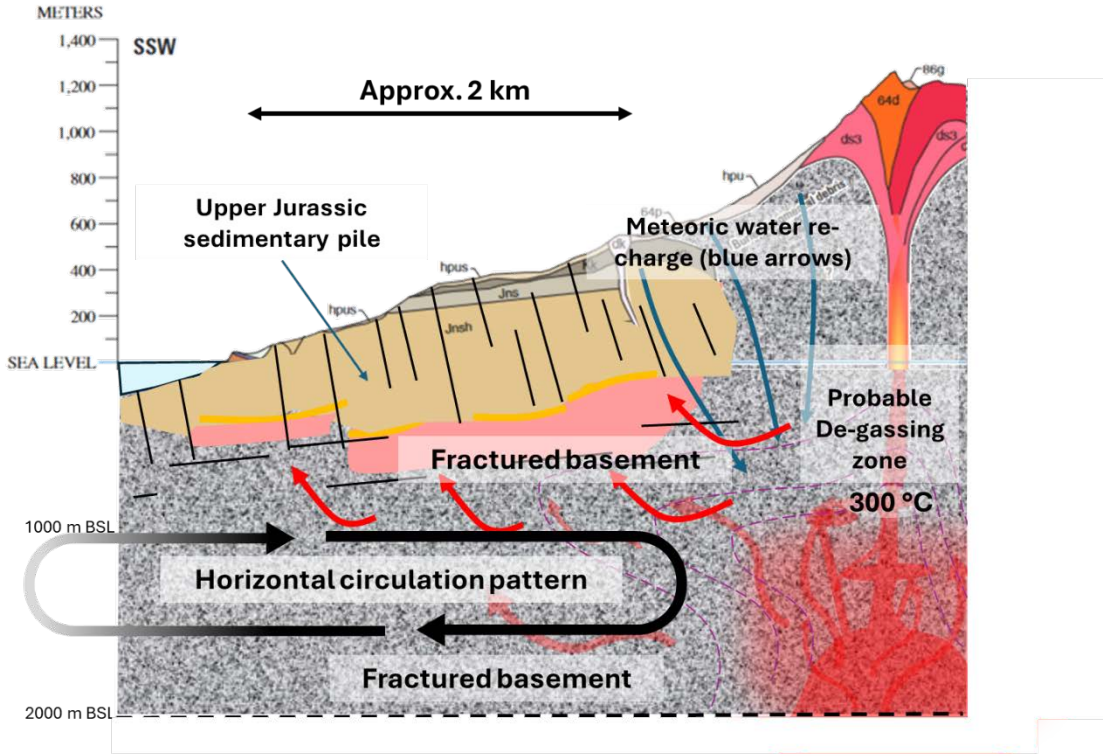

Figure 9: Geological model of potential geothermal resource under the southern flank of Augustine Volcano. See text for further information (modified from Waitt and Begét, 2009, see reference for acronym explanation).

The combined resistivity and density data from the 3D AMT/gravity datasets corroborates the above findings. The convergence of low resistivity and high density volumes on the southern flank of the island represents the Upper Jurassic sediment seal or geothermal clay cap sitting above a higher zone of resistivity which is likely to represent the hydrothermal system. (Figure 10).

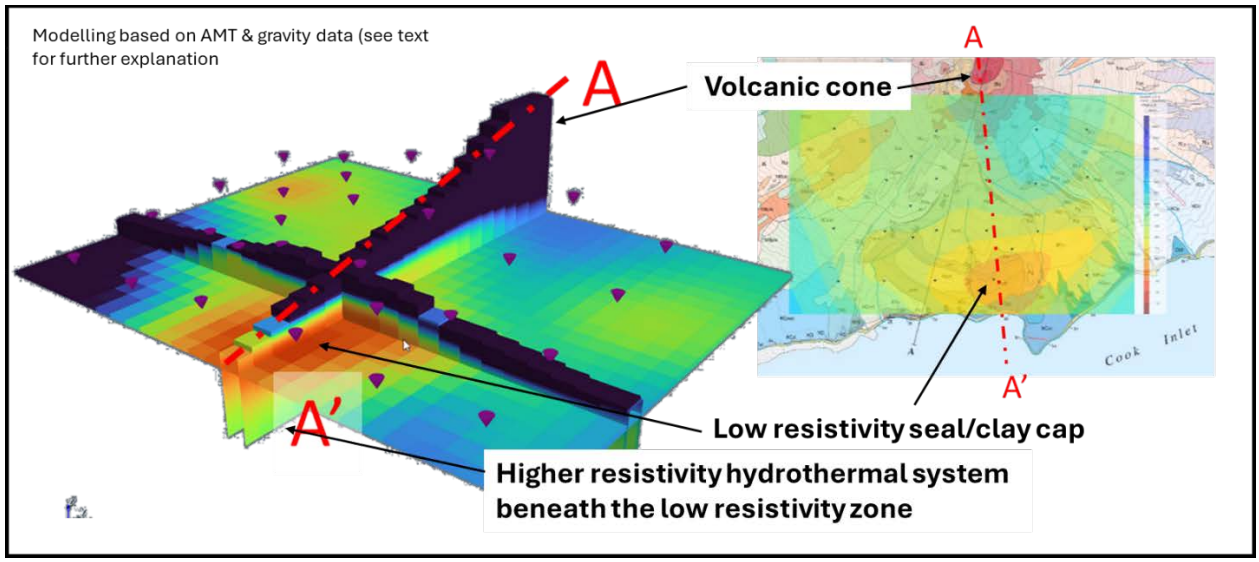

Figure 10: 3D modelling of AMT and Gravity data revealing a volume of low resistivity and high-density within the southern part of Augustine Island

5.2 Seismic model

In all vertical sections a strong anomaly of very high dV_P was observed within the edifice of the volcano which is interpreted as the igneous rock structure within the edifice (see Figure 8, point a). Conversely a very low dV_S was observed within the edifice which can be interpreted as fractures filled with fluids and melts (see Figure 8, point b). Also, the data reveals a high dV_P, low to moderate dV_S columnar anomaly associated with high dV_P/dV_S observed at a greater depth below the edifice which is interpreted as a slender magma conduit (see Figure 8, point c). In addition, a sudden change in dV_P/dV_S from high to low values is observed between the edifice and the magma conduit. This behavior is associated with high, dense seismicity and could be the result of a zone of degassing region (see Figure 8, point d).

The Southern flank of Mt Augustine represents a high potential for geothermal resource development. In section 1A-1B we observe the presence of a columnar anomaly of relatively high dV_P, high dV_s and relatively low dV_P/dV_S (see Figure 8, point e). This anomaly could be interpreted as a brittle zone where degassed fluids form fractures and quickly propagate upwards (Koulakov et al., 2023a). Also, in section 1A-1B both dV_P and dV_S increase as we go further away from the shoreline (see Figure 8, point f to g). This increase could be due to the decrease in the saturation of water further away from the shoreline. Aside from the magma conduit and edifice, the Upper Jurassic silts and sands were observed to have a higher V_P and V_S. This observation coincides with the theory of having a thermally altered clay layer that works as a seal between the fractured saturated basement below and the silts and sands, above. Similar anomalies were observed for section 4A-4B and the interpretation of these anomalies is the same.

In section 2A-2B, a relatively high dV_P associated with low dV_S which results in high dV_P/dV_S anomaly is observed under the southern flank of the volcano (see Figure 8, point h). Our interpretation is that dV_P is less in this region because of the Upper Jurassic sedimentary lithology (Takei, 2002; Waitt and Begét, 2009) when compared to the igneous structure of the edifice. On the other hand, another reason for dV_P to increase is the presence of water. This assumption is verified by the low dV_S and high dV_P/dV_S in the area (Adam and Otheim, 2013).

Combining the geological, resistivity, gravity and seismic data, the basis of a working hydrothermal system is identified under the southern flank of Augustine Volcano (Figure 11). The geological, resistivity and gravity data support the identification of an effective seal/clay cap, while the seismic data identifies a fluid filled zone of fractured basement directly beneath this. The areal extent of the seal/clay cap has been calculated as 3000 m^2 while the underlying hydrothermal resource volume has been calculated as 1,200,000 m^3 (based upon currently available data).

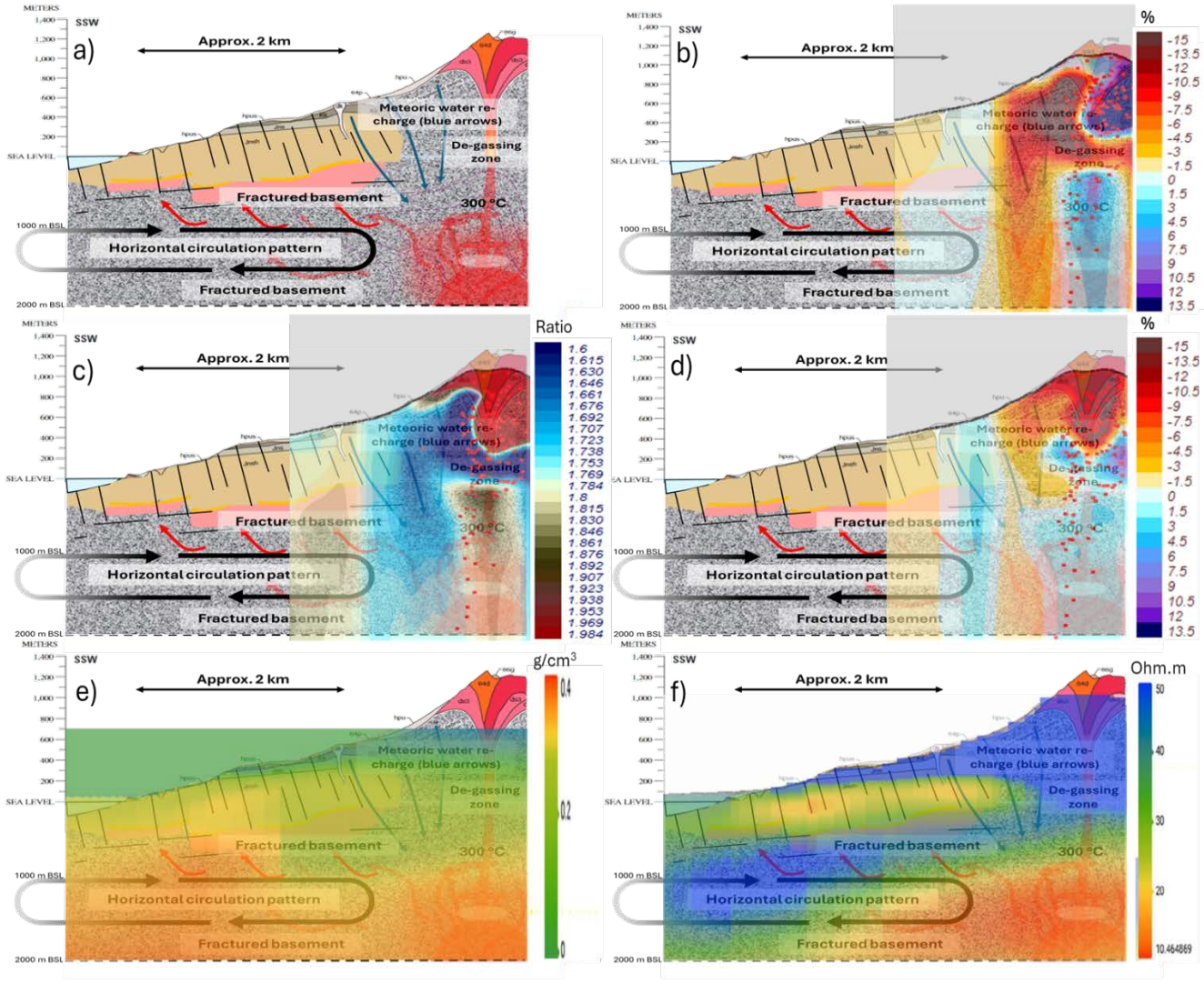

Figure 11: Full sub-surface model combining the (a) geologic model with (b) dV_P, (c) dV_P/dV_S, (d) dV_S, (e) gravity and (f) AMT data.

5.3 Discussion

Due to the presence of the Jurassic seal/clay cap, we describe this geothermal resource as 'atypical'. A typical geothermal resource on a volcanic flank normally requires hydrothermal alteration of volcanic sediment/basement in order to create an effective seal. In addition, and due to the absence of identified surface manifestations, the potential geothermal resource identified at Augustine Volcano could be described as 'blind'. Blind geothermal systems are hydrothermal systems that lack surface thermal features (*e.g.* hot springs, mud volcanoes, *etc*). However, they share many features in common with conventional identified hydrothermal systems. Dobson, 2016 identifies a number of geologic factors that could prevent the rise of hot, buoyant fluids from reaching the surface including,

- Blind systems may have thicker, better developed seals
- Faults associated with blind systems may not reach the surface or may be fault-sealed
- Blind systems may contain depressed water tables that result in no surface thermal manifestations
- Blind systems may be obscured by an overlying cold-water aquifer
- Blind systems may be smaller than identified hydrothermal systems in the same geologic setting
- Blind systems may be deeper than their identified geothermal counterparts

There are good examples of blind geothermal systems located in volcanic zones that have been developed for geothermal power production including Puna Geothermal Venture, Hawaii and Cerro Pabellón Geothermal Field, Chile. Cerro Pabellón is located in a subduction zone volcanic center and is located on the eastern flank of the Apacheta volcano, and thus has a similar geological setting to Mt. Augustine. A thick altered clay seal consisting of smectite-illite mix has formed over the geothermal reservoir, blocking any vertical migration of fluids, thus resulting in a dominant horizontal circulation pattern (Maza *et al.*, 2021, Baccarin *et al.* 2021). Despite the lack of surface manifestations, Cerro Pabellón geothermal system has a current installed power capacity of 83 Mwe.

Based on the data collected from Augustine Volcano to date, we believe that the potential identified geothermal resource shows many similarities with Cerro Pabellón which could represent a good analogue for future development.

6. Volumetrics and Uncertainties

Based on the results from the seismic, AMT, gravity, and geological data, a potential hydrothermal resource was identified in the southern part of the island and within the original permit area. In order to volumetrically evaluate this potential hydrothermal resource, two reservoir estimation methods (the volumetric method and the power density method) were evaluated.

The volumetric method is widely used to quantify geothermal resource capacity. Equation 1 is used to estimate the megawatts of electric power that can be generated from a geothermal resource (Muffler, 1979). Equation 2 is used to determine the thermal energy (q) measured in joules (J) (Garg and Combs, 2015; Muffler and Cataldi, 1978).

$$MWe = \frac{qXR_fX\eta_{\text{conv}}}{FXL} \quad (1)$$

$$q = q_r + q_f = Ah(T_i - T_f)[(1-\varphi)\rho_R c_R + \varphi(X_L \rho_L c_L + X_V \rho_V c_V) \quad (2)$$

X_L and X_V can be calculated using Equation 3 (O'Sullivan and O'Sullivan, 2016). While the rock is considered fully saturated where $X_L + X_V = 1$ and their entropies are obtained using the steam tables for two-phase saturated fluid. All the variables and their units are summarized in Table 3.

$$X_V = \frac{S_{L@Ti} - S_{L@Tr}}{S_{V@Tr} - S_{L@Tr}} \quad (3)$$

Table 3: Variables and corresponding units for parameters used in Equations 1 through 3.

Symbol	Name	Unit
MWe	Power Potential	Mwe
Q	Thermal energy	MJ
R_f	Recovery factor	%
L	Power plant lifespan	Seconds
η_{conv}	Conversion factor	%
F	Load factor	%
A	Area	m^2
H	Thickness	m
T_i	Initial reservoir temperature	°C
T_r	Reference Temperature	°C
T_f	Final abandonment temperature	°C
$\rho_i c_i$	Volumetric heat capacity	$J/m^3°C$
X_L	Liquid fraction	%
X_V	Vapor fraction	%
S_L	Entropy of liquid phase	J/K
S_V	Entropy of vapor phase	J/K

The power density method is another way to estimate potential power generation per area (Mwe/Km^2). The simple calculation and the few assumptions for power density make it a favorable choice especially in an early exploration phase. Wilmarth and Stimac, (2015) have developed Figure 12 for 53 geothermal fields based on tectonic settings in correlation with reservoir temperature.

Based on the current dataset, potential power generation was calculated using both power density and volumetric methods and averaged for further calculations. Since there are a lot of uncertainties associated with any green field prospect like Mt Augustine, Monte Carlo simulation (MCS) with 10,000 iterations was utilized to reduce the level of uncertainty. Figure 13 shows the histogram distribution for the potential MWe for Mt Augustine. The P_{50} has been calculated as 70 MWe with a P_{90}-P_{10} range of 49 MWe to 93 MWe. These numbers will change as GeoAlaska collects additional quantitative data.

Once the power production potential is calculated it can then be used to estimate the number of wells required to effectively produce the resource. The MWe/number of wells is assumed to be 3.5 MWe/well for slim wells (Alarcón, 2023) and 8.5 MWe/well for conventional wells, both of which agree with the Cerro Pabellón Field full field development plan (Lobos Lillo et al., 2023). Tables 4 and 5 summarize all the key data and assumptions used in the power production potential calculation. Once the optimum number of wells is calculated, the technical assessment is concluded, and the economic assessment can commence.

Based on the current dataset and the results of the volumetric modelling, the optimal number of wells required to develop the prospect is 11 conventional wells or 27 slim wells.

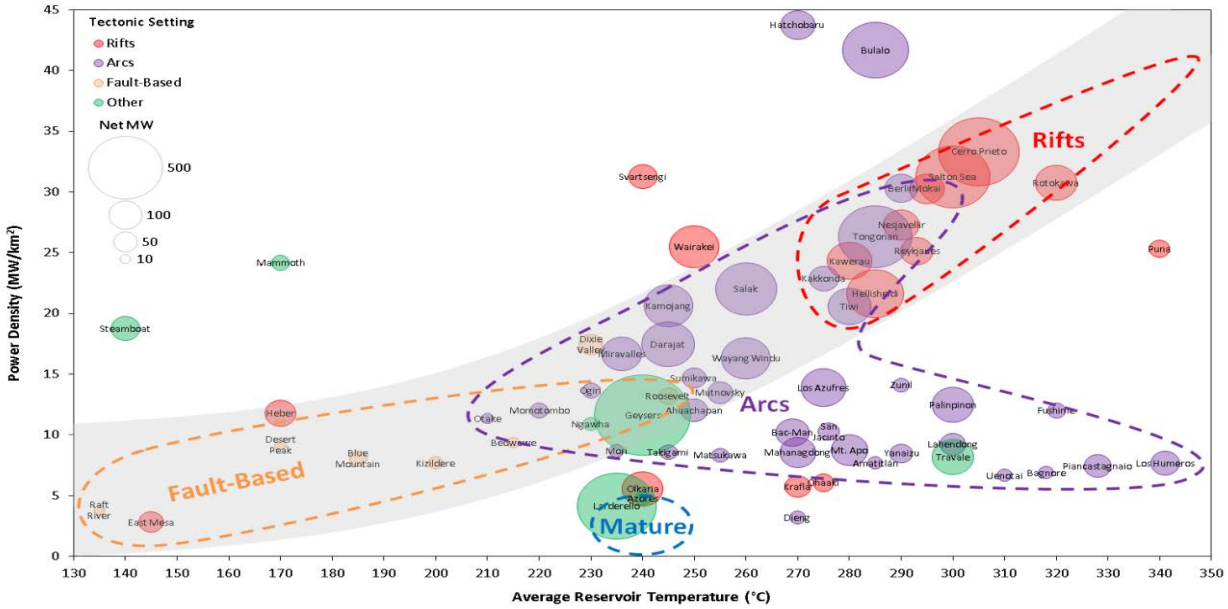

Figure 12: Clusters of geothermal wells and the correlation of their power density with measured reservoir temperature, (Wilmarth and Stimac, 2015).

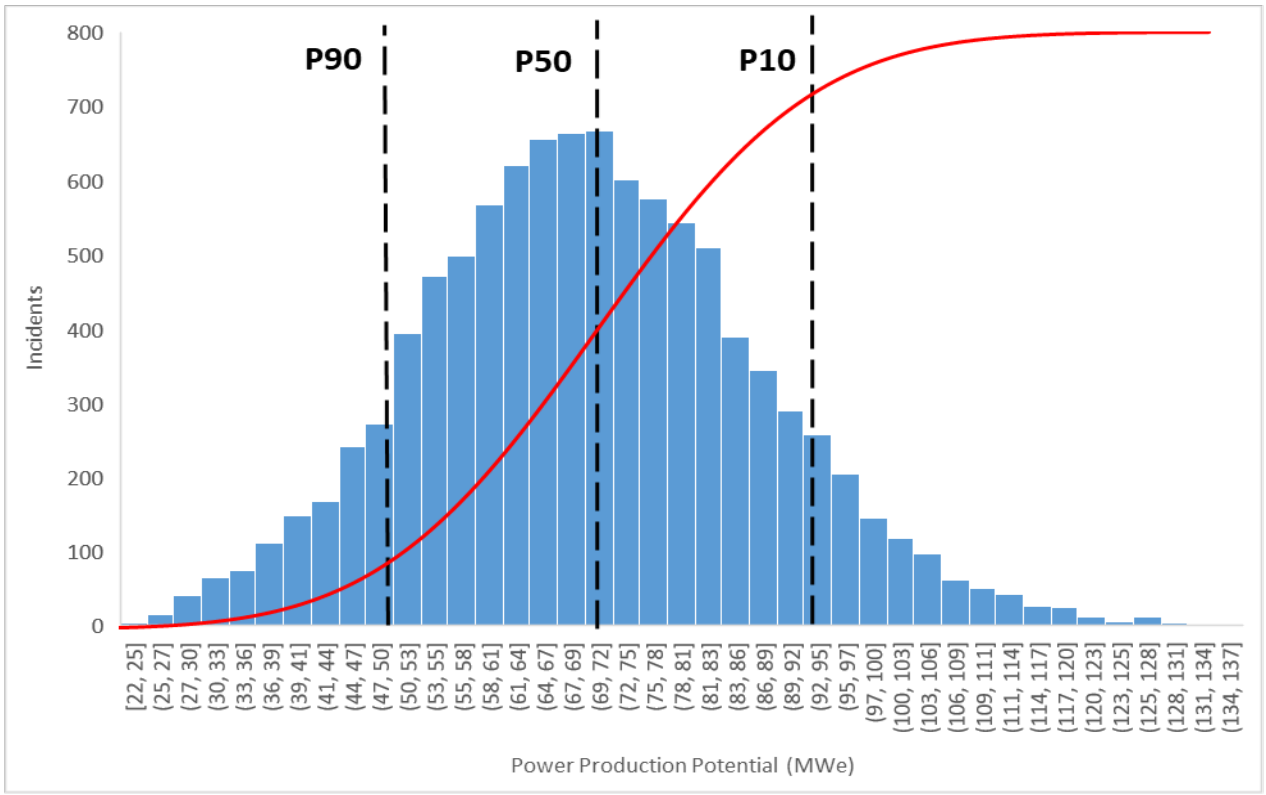

Figure 13: MCS histogram distribution for power production potential in MWe. 70 MWe is the P50 and a P90-P10 range of 49 MWe to 93 MWe. CDF is the cumulative distribution function of power production potential to be equal a certain value or less.

Table 4: Summary of the variable data utilized for MCS modelling.

Parameter	Most Likely	Minimum	Maximum	Unit	Reference
Rock porosity (φ)	10	5	15	%	(Ciriaco et al., 2020)
Recovery Factor (Rf)	15	5	20	%	(Garg and Combs, 2015)
Conversion efficiency (η_{conv})	75	70	80	%	(Garg and Combs, 2015)
Abandonment temperature (T_f)	100	100	151.831	°C	(Aravena et al., 2016)
Area	3.5	3	4	Km^2	2023 AMT Data
Thickness	400	200	600	m	2023 AMT Data
Production decline rate	0.15	0	0.5	%	(Alarcón, 2023)
Cost Increase rate	2	0	10	%	(Alarcón, 2023)
Power Density range	15	10	25	MWe/Km2	(Wilmarth and Stimac, 2015)

Table 5: Summary of the fixed data utilized for MCS modelling.

Parameter	Value	Unit	Reference
Reference Temperature	15	°C	(Sanyal et al., 2004) (Williams 2004) (Basel et al. 2010)
Initial Reservoir Temperature	280	°C	(Eichelberger et al. 2023)
Volumetric heat capacity of the rock ($\rho_R c_R$)	2700	$KJ/m^3°C$	(Aravena et al., 2016)
Lifespan (L)	30	Years	(Ciriaco et al., 2020)
Capacity factor (F)	95	%	(Aravena et al., 2016)

The economic assessment assumes the delivery of electrical power to the shoreline of Mt. Augustine and does not consider transfer of power to the mainland. It is divided into three main parts, CAPEX, OPEX and Revenue. Firstly, CAPEX can be divided into development costs and construction costs. The development cost includes surface exploration, project management, testing and reservoir management, infrastructure (well pads, etc.), drilling of production wells, drilling of injection wells, design and engineering, land, permitting, environmental management and contingency reserve. The construction cost includes powerplant engineering, procurement and construction (EPC), insurance, management and others (Martínez Ruiz et al., 2022; Osorio Luna, 2018). Powerplant EPC can be calculated using Equation 4 (Martínez Ruiz et al., 2022; Sanyal, 2005).

$$EPC = KW * CC = KW * CPP * e^{-0.0025(MW-5)} \quad (4)$$

Where, CC is the capital cost in USD/kW, CPP is the cost per kW of the powerplant, and W is the gross power output of the power plant in MW. The cost per kW of the powerplant (CPP) varies depending on the type of powerplant and any changes in the technologies involved. CPP ranges between 1,700 USD/kW to 2000 USD/kW (Alarcón, 2023).

OPEX calculations also include such costs as insurance, easements, concession leases, selling and administrative expenses, environmental mitigation, utilities, auxiliary power, OandM externalization and royalties. The net potential generation capacity is calculated by subtracting the parasitic loads shown in Table 6 from total potential capacity. Based on Table 6 calculations, the net potential generation capacity is 89% of the total potential capacity.

Based on the current dataset and assumptions the economic modelling predicts a total CAPEX investment to range from \$181 to \$287 million USD as P_{10} and P_{90}, respectively. P_{50} for total CAPEX is \$234 million USD which represents a 3.4 million USD/MWe CAPEX investment per power generation. Figures 15 shows the range of P10 to P90 for CAPEX investment per MWe.

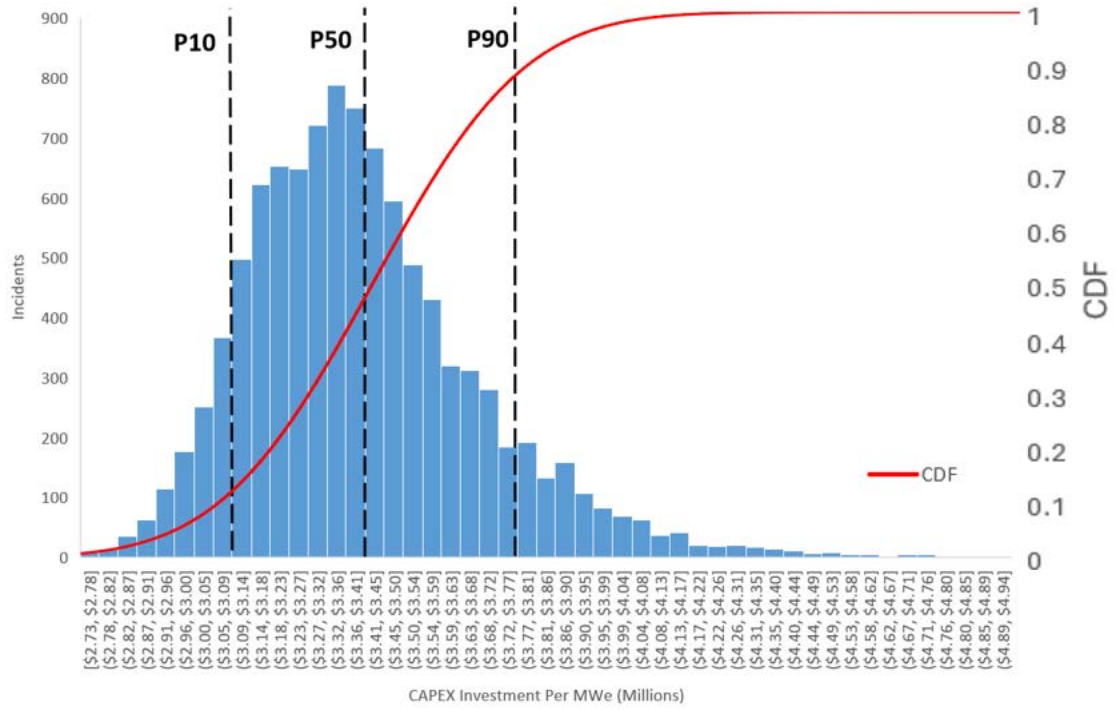

Figure 15: MCS histogram distribution for CAPEX investment per MWe. \$3.4 million /MWe is the P50 while P90-P10 range from \$3.1 to \$3.8 million/MWe. CDF is the cumulative distribution function of CAPEX investment per MWe to be equal a certain value or less.

7. Full Field Development Plan

Any development efforts are accompanied by an underlying business plan that relies on carefully derived assumptions and is updated as new information is revealed. Economic evaluation criteria include the internal rate of return (IRR) and net present value (NPV). Current assumptions in determining the viability of this project neglect beneficial tax breaks, carbon offset credits, and debt leverage from project finance. The location also warrants high capital expenditure and operating cost to mitigate against geohazards, as well as costs associated with the remote location. Finally, the financial calculations assume a zero-terminal value for the power plant after 35 years even though other geothermal plants around the world operate long after their design life spans., Figure 16 plots undiscounted cumulative net cash flow for the full project life cycle versus time.

Lastly, an overview of the full evaluation process for Mt Augustine is presented in Figure 18 and Table 7.

Based on the results obtained from the full field evaluations, the payout time for Mt Augustine is between the year 2034 to 2035, assuming a start date of January 1st 2022. The IRR for the project has an 80% probability to be between the range of 16.44% and 20.42% with P50 equal to 18.48%. Figure 17 show the histogram distribution for IRR as it calculates today.

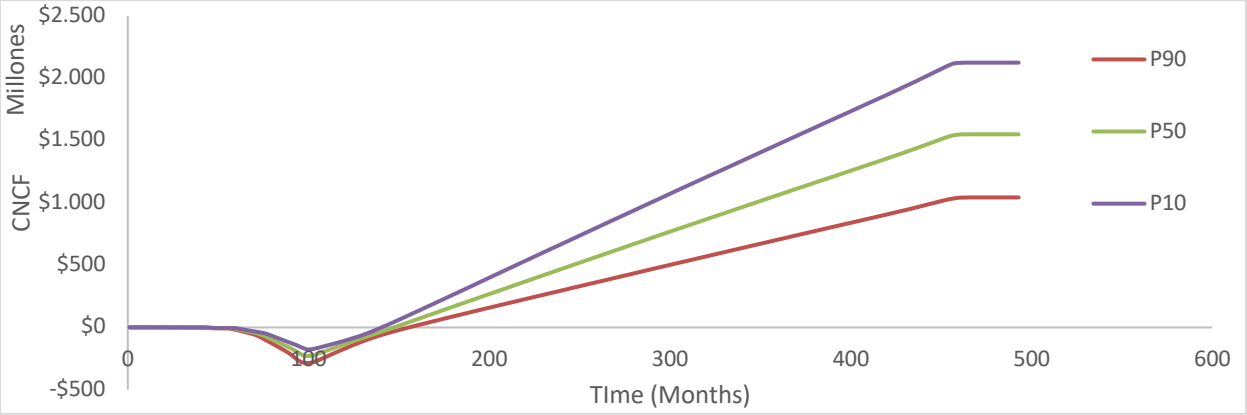

Figure 16: Undiscounted CNCF before tax versus time for different scenarios.

Table 6: Summary of the parasitic loads (Alarcón, 2023).

Type of Load	Percentage of the total capacity
Average powerplant consumption	6%
Average reinjection pumps	2.75%
Average contingency systems	2.25%
Total	11.00%

Table 7: Summary of the undiscounted economic results before tax, credits, depreciation, and project finance considerations.

Output	10%	50%	90%
Total Installed CAPEX	$ 181,496,071	$ 233,861,921	$ 287,315,152
Net Power Production Potential (MWe)	49	70	93
Number of Wells	8	11	14
Number of Slim Wells	18	27	36
CAPEX Investment Per MW	$ 3,091,623	$ 3,402,422	$ 3,771,093
IRR (35 Years)	16.44%	18.48%	20.42%
NPV (35 Years)	$ 71,403,695	$ 126,446,230	$ 185,064,641
Payout (Months)	140	147	155

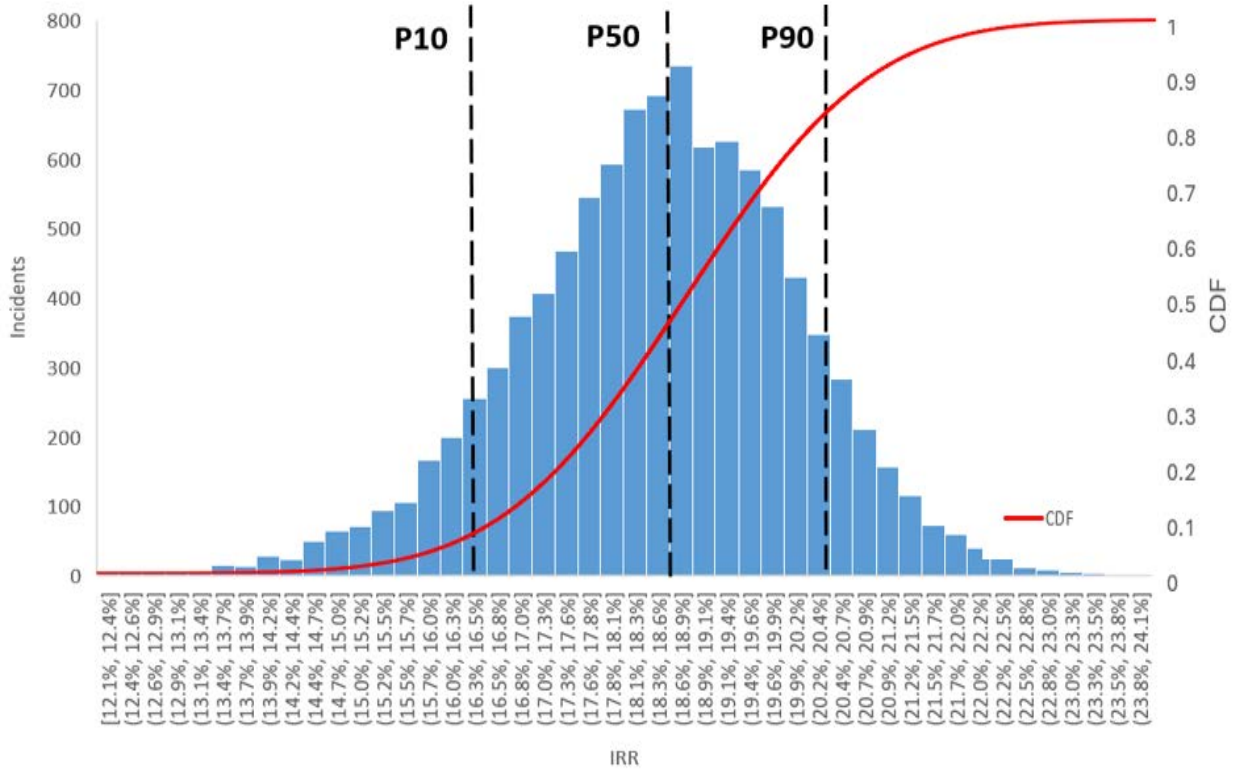

Figure 17: MCS modelling histogram distribution for IRR after 35 years. 18.48% is the P50 while P90-P10 range from 16.44 to 20.42%. CDF is the cumulative distribution function of IRR to be equal a certain value or less.

8. Next Steps

Figure 19 displays GeoAlaska's plans for exploration, appraisal. and development of the Augustine Volcano's potential geothermal resource. Our aim is to contribute to a 24/7 reliable baseload energy supply for Alaskans residing within the Railbelt Region of Southcentral Alaska.

GeoAlaska has commissioned additional MT data collection, processing and 3D modelling to further resolving the depth to base of the Jurassic seal, and the volume of the potential hydrothermal system identified from the 2023 dataset. GeoAlaska has expanded the survey area with the recent lease expansion; additional data will be collected across the entire south of Augustine Island to delineate the spatial extent of this and other potential prospects. During 2025, GeoAlaska intends to drill its first exploration well, the location of which will be determined by the results of the MT data analysis. The intention of the exploration well will be to penetrate beyond the base of the Jurassic seal and into the reservoir to gain information on the reservoir, fluid type, fluid flow, and temperature. This data should enable GeoAlaska to improve plans for development drilling.

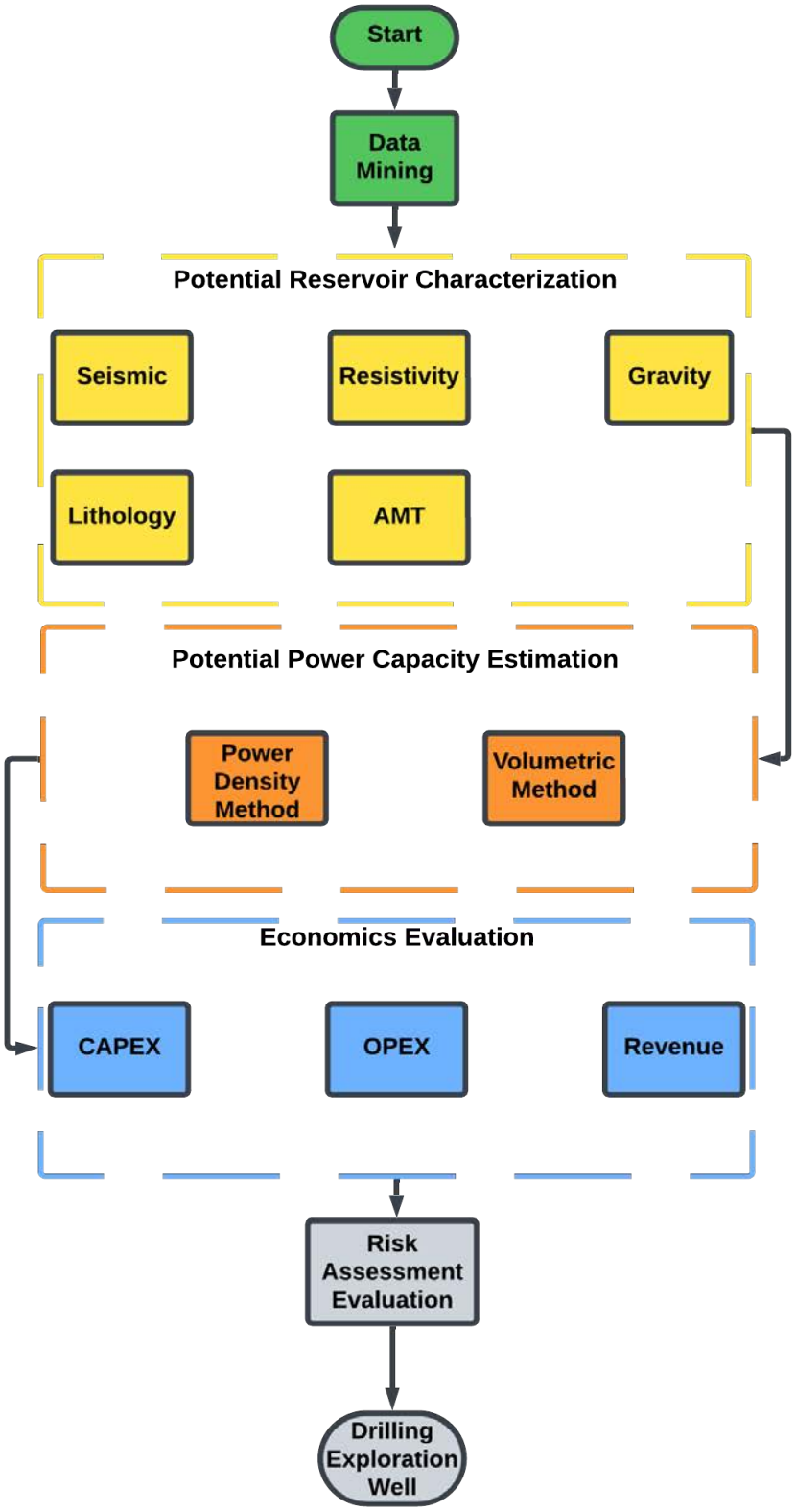

Figure 18: Mt Augustine full evaluation process.

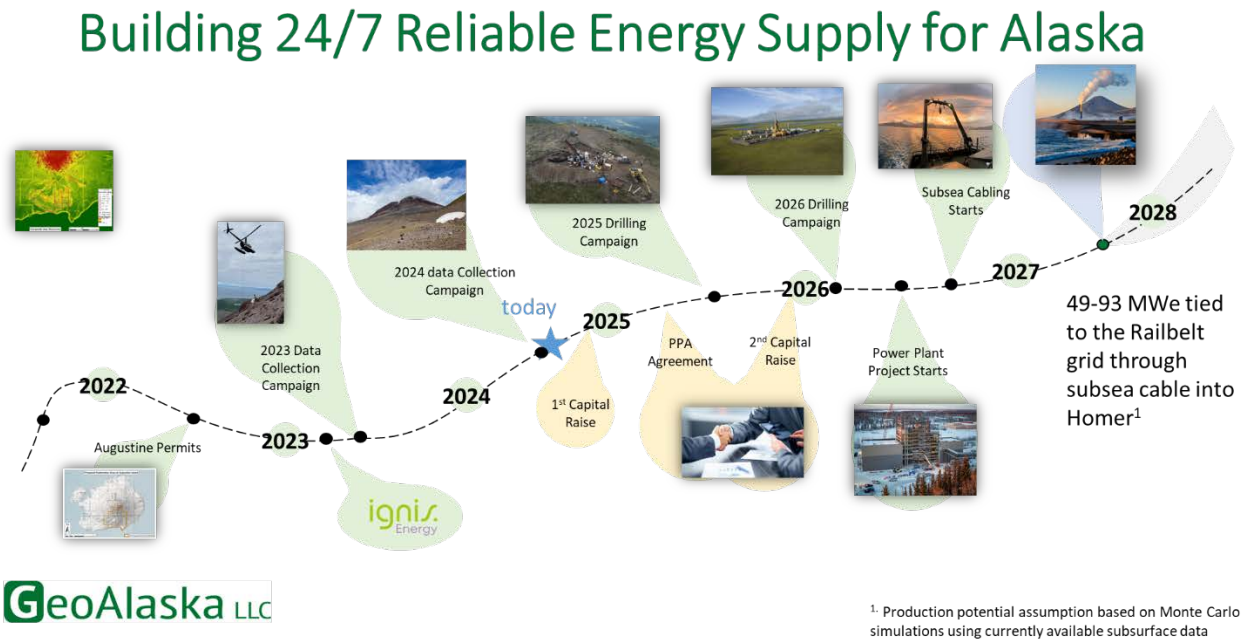

Figure 19: Expected exploration, appraisal and development timeline for Augustine Volcano geothermal project.

9. Conclusions

1. Augustine Volcano (Mt. Augustine) is an active stratovolcano located in the southwestern Cook Inlet, Southcentral Alaska, approximately 60 miles west of Anchor Point, Kenai Peninsula, and adjacent to the Railbelt Region of Alaska which houses approximately 550,000 residents whose current power generation is dominated by natural gas and coal.
2. The Governor of Alaska recently requested a study on the potential impacts of achieving an 80% renewable energy portfolio for Southcentral Alaska including any potential geothermal resource.
3. Since 2021, GeoAlaska and its partner Ignis Energy have permitted 10,830 acres and extended the original lease holding on the southern flank of Mt Augustine, with a view to explore its full geothermal potential.
4. Outcropping on the southern flank of the island are a series of silt-grade to coarse-grained Upper Jurassic Naknek Fm. sediments. Outcrop studies confirmed that these sediments can contain up to 29% smectite.
5. During the summer of 2023, AMT and Gravity data were collected over a portion of the southern flank of the island, corresponding to the first tract of geothermal prospecting permits.
6. Inversion and 3D modelling of these data suggest the presence of a low resistivity and high density seal or clay cap, corresponding to the Upper Jurassic sub-crop overlying a zone of higher resistivity which is likely to represent the underlying hydrothermal system. Based on these data, the area of the clay cap is measured at 3 km^2, while the thickness of the underlying reservoir is thought to be around 400 m.

7. GeoAlaska utilized catalog seismic data provided by the Alaska Volcano Observatory. These data corroborate the identification of a sedimentary clay cap overlying a fluid-filled zone of fractured basement.
8. Based on the assumed reservoir temperature of 280° C and all other assumptions, the potential power production was estimated using two methods, the volumetric method and the power density method. A Monte Carlo simulation predicts a P50 of 70MWe and a range (P90-P10) of 49MWe to 93MWe.
9. According to the above-mentioned economic analysis the development of Mt Augustine will require around 3.4 million USD per MWe. The IRR ranges between 16.44% to 20.42% with a payout time of 12 years from project start.
10. GeoAlaska continues to collect additional sub-surface data as a means of further de-risking the geothermal prospect(s) and to identify a suitable location to drill its first exploration well during 2025.

Acknowledgements

GeoAlaska and its partner Ignis Energy would like to acknowledge and thank the following, all of whom have assisted and contributed significantly to this project to-date:

Alaska Oil and Gas Conservation Commission (AOGCC)

Alaska Volcano Observatory (AVO)

Logic Geophysics and Analytics

Pollux Aviation Ltd.

JRG Energy Consultants Ltd.

Geolog International B.V.

Geotech labs, Milan (a Division of Geolog International B.V.)

Texas AandM University

Professor Nathan Meehan (Harold Vance Department of Petroleum Engineering, Texas AandM University) and Danny Rehg (VP Operations, Ignis Energy Inc.) both of whom provided valuable and constructive comments on the content of this manuscript.

REFERENCES

Adam, L., Otheim, T., 2013. Elastic laboratory measurements and modeling of saturated basalts. *JGR Solid Earth 118*, 840–851. https://doi.org/10.1002/jgrb.50090

Alarcón, A.I.M., 2023. Technical, economic, social, and environmental assessment of geothermal resources in Chile.

Asmus, P., Rogers, B., Cicilio, P., Colt, S., Burtness-Adams, F. and Hansen, J., 2023. Railbelt Decarbonization Pathways Study Public Comment Summary. *Alaska Center For Energy and Power Technical Report* UAF/ACEP/TP-01-001, June 2023.

Buffler, R., 1976. Geologic map of south Augustine Island, lower Cook Inlet, Alaska. *Alaska Department of Natural Resources, Division of Geology and Geophysical Surveys*, Open-File Report AOF-96, 3 pages and map.

Ciriaco, A.E., Zarrouk, S.J., Zakeri, G., 2020. Geothermal resource and reserve assessment methodology: Overview, analysis and future directions. *Renewable and Sustainable Energy Reviews 119*, 109515. https://doi.org/10.1016/j.rser.2019.109515

Garg, S.K., Combs, J., 2015. A reformulation of USGS volumetric "heat in place" resource estimation method. *Geothermics 55, 150–158.*

Dahlstrom, N., Thayer, C. and Koplin, C, 2023. *Alaska Energy Security Task Force Report, Volume 1*.

Detterman, R. and Jones, D., 1974. Mesozoic fossils from Augustine Island, Cook Inlet, Alaska. *American Association of Petroleum Geologists Bulletin, v. 58*, pages 868-870.

Detterman, R. and Reed, B., 1964. Preliminary map of the geology of the Iliamna quadrangle, Alaska. U.S. *Geological Survey Miscellaneous Investigations Map I-407, scale 1:250,000*.

Dobson, P., 2016. A review of exploration methods for discovering hidden geothermal systems. *Geothermal Rising Conference Transactions, Vol. 40*, 2016, pages 695-706.

Eichelberger, J., Foster, M. and Holdmann, G., 2023. Augustine Volcano, Cook Inlet, Alaska has Magma Storage at Shallow Depth and Merits Geothermal Exploration. *Geothermal Rising Conference Transactions, Vol. 47*, 2023

ENSTAR, 2024. Cook Inlet Update Report, February 7th, 2024.

Erkan, K., Holdmann, G., Benoit, W. and Blackwell, D, 2008. Understanding the Chena Hot Springs, Alaska, geothermal system using temperature and pressure data from exploration boreholes. *Geothermics, Volume 77*, Issue 6, December 2008, pages 565-585.

Evans, W.C., Bergfeld, D., Neal, C.A., McGimsey, R.G., Werner, C.A., Waythomas, C.F., Lewicki, J.L., Lopez, T., Mangan, M.T., Miller, T.P. and Diefenbach, A., 2015. Aleutian Arc Geothermal Fluids: Chemical Analyses of Waters and Gases Sampled in Association with the Alaska Volcano Observatory. *US Geol. Surv. Data Release*.

Goodfellow, P. and Birnbaum, M., 2023. Alaska Greenhouse Gas Emissions Inventory 1990-2020. *Alaska Department of Environmental Conservation Division of Air Quality*, May 25, 2023 report.

Hinga, B.D.R., 2015. Ring of Fire: An Encyclopedia of the Pacific Rim's Earthquakes, Tsunamis, and Volcanoes. *Bloomsbury Publishing USA*.

Haeussler, P., Bruhn, R. and Pratt, T., 2000. Potential seismic hazards And tectonics of the upper Cook Inlet basin, Alaska, based in analysis of Pliocene and younger deformation, IN. *Geological Society of America Bulletin, Vol. 112, Issue 9*, pages 1414 – 1429.

Herriott, T., Wartes, M. and Decker, P., 2016. Record of a late Jurassic deep-water canyon at Chisik Island, Southcentral Alaska: Further delineation of Naknek Formation depositional

systems in Lower Cook Inlet. In, Herriott T. (ed), Petroleum-related geologic studies in lower Cook Inlet during 2015, Iniskin-Tuxedni region, Southcentral Alaska: *Alaska Division of Geological and Geophysical Surveys Preliminary Interpretative Report 2016-1*, 78 pages.

Kamata, H., Johnston, D.A., Waitt, R.B., 1991. Stratigraphy, chronology, and character of the 1976 pyroclastic eruption of Augustine volcano. *Alaska. Bulletin of Volcanology 53*, 407–419. https://doi.org/10.1007/BF00258182

Koulakov, I., 2009. LOTOS Code for Local Earthquake Tomographic Inversion: Benchmarks for Testing Tomographic Algorithms. *Bulletin of the Seismological Society of America 99*, 194–214. https://doi.org/10.1785/0120080013

Koulakov, I., D'Auria, L., Prudencio, J., Cabrera-Pérez, I., Barrancos, J., Padilla, G.D., Abramenkov, S., Pérez, N.M., Ibáñez, J.M., 2023a. Local Earthquake Seismic Tomography Reveals the Link Between Crustal Structure and Volcanism in Tenerife (Canary Islands). *JGR Solid Earth 128*, e2022JB025798. https://doi.org/10.1029/2022JB025798

Koulakov, I., Qaysi, S.I., Izbekov, P., Browne, B.L., 2023b. Structure of shallow magma sources beneath Augustine Volcano (Alaska) inferred from local earthquake tomography. *Journal of Volcanology and Geothermal Research 444*, 107965.

Koulakov, I.Yu., 2020. BASIC TOMO: an educational tool for investigating the role of controlling parameters and observation geometry in tomography problems. *Russian Journal of geophysical technologies 40–54*. https://doi.org/10.18303/2619-1563-2020-1-40

Lobos Lillo, D., Delgado, F., Pritchard, M.E., Cardona, C., Franco, L., Pedreros, G., Amigo, A., 2023. Documenting surface deformation at the first geothermal power plant in South America (Cerro Pabellón, Chile) by satellite InSAR time-series. *Journal of Volcanology and Geothermal Research 441*, 107869. https://doi.org/10.1016/j.jvolgeores.2023.107869

Martínez Ruiz, Y., Duque, D.F.M., Ramírez Malule, H., 2022. Geothermal Power Projects Valuation Model, in: García Alcaraz, J.L., Realyvásquez Vargas, A. (Eds.), *Algorithms and Computational Techniques Applied to Industry*. Springer International Publishing, Cham, pp. 29–46. https://doi.org/10.1007/978-3-031-00856-6_2

Maza, S., Collo, G., Morata, D., Taussi, M., Vidal, J., Mattioli, M., and Renzulli, A., 2021. Active and fossil hydrothermal zones of the Apacheta volcano: Insights for the Cerro Pabellón hidden geothermal system (Northern Chile). *Geothermics, 102206*.

Muffler, L.J.P., 1979. Assessment of geothermal resources of the United States, 1978 (No. USGS-CIRC-790). *Geological Survey, Reston, VA (USA). Geologic Div.* https://doi.org/10.2172/6870401

Muffler, P., Cataldi, R., 1978. Methods for regional assessment of geothermal resources. *Geothermics 7*, 53–89. https://doi.org/10.1016/0375-6505(78)90002-0

Osorio Luna, G.E., 2018. Análisis de sinergias en la minería de la región de Antofagasta (Master's). Pontificia Universidad Catolica de Chile (Chile), Chile.

O'Sullivan, M.J., O'Sullivan, J.P., 2016. 7 - Reservoir modeling and simulation for geothermal resource characterization and evaluation, in: DiPippo, R. (Ed.). *Geothermal Power Generation. Woodhead Publishing,* pp. 165–199. https://doi.org/10.1016/B978-0-08-100337-4.00007-3

Power, J.A., Nye, C.J., Coombs, M.L., Wessels, R.L., Cervelli, P.F., Dehn, J., Wallace, K.L., Freymueller, J.T., Doukas, M.P., 2006. The reawakening of Alaska's Augustine volcano. *EoS Transactions 87*, 373–377. https://doi.org/10.1029/2006EO370002

Sanyal, S.K., Klein, C.W., Lovekin, J.W. and Henneberger, R.C., 2004. National assessment of US geothermal resources-a perspective. *Geothermal Resources Council Transactions, 28*, pp.355-362.

Sanyal, S.K., 2005. Cost of Geothermal Power and Factors that Affect It.

Swanson, S.E., Kienle, J., 1988. The 1986 Eruption of Mount St. Augustine: Field Test of a Hazard Evaluation. *J. Geophys. Res. 93*, 4500–4520. https://doi.org/10.1029/JB093iB05p04500

Syracuse, E.M., Thurber, C.H., Power, J.A., 2011. The Augustine magmatic system as revealed by seismic tomography and relocated earthquake hypocenters from 1994 through 2009. *J. Geophys. Res. 116*, B09306. https://doi.org/10.1029/2010JB008129

Takei, Y., 2002. Effect of pore geometry on V P / V S : From equilibrium geometry to crack. *Journal of Geophysical Research 107.* https://doi.org/10.1029/2001JB000522

U.S. Energy Information Administration, 2022. Geothermal explained. Where geothermal energy is found. Update February 15th, 2022.

U.S. Energy Information Administration, 2024. State Profile and Energy Estimates Overview. Update April 18th, 2024.

U.S. Energy Information Administration, 2024. Electric Power Monthly, Table 5.6.A, average price of electricity to ultimate customers by end-use sector. Update March 2024.

Waitt, R.B., Begét, J.E., 2009. Volcanic processes and geology of Augustine Volcano, Alaska. *U.S. Geological Survey Professional Paper, 1762*, 78 p., 2 plates, scale 1:25,000.

Waythomas, C. and Waitt, R., 1998. Preliminary volcano-hazards assessment for Augustine Volcano, Alaska. *U.S. Geological Survey Open-File Report 98-106*, 39 pages.

Wilmarth, M., Stimac, J., 2015. Power Density in Geothermal Fields. *Proceedings World Geothermal Congress 2015.* Melbourne, Australia 19-25 April

Addendum to paper

2024 update

During the summer of 2024, an additional 40 standard MT measurements were collected across the entire permit area on the southern part of Augustine Island (Figure i) to further compliment the data collected during 2023.

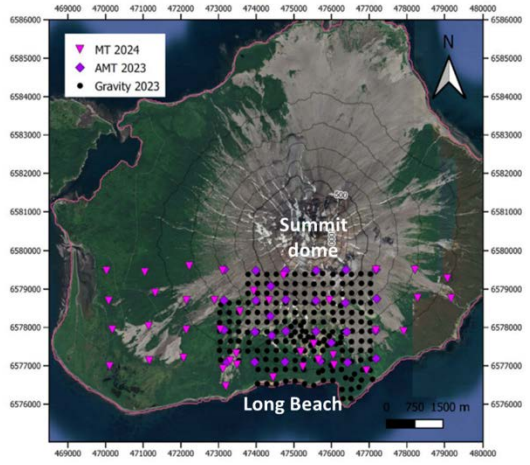

Figure i. AMT, MT & Gravity sampling locations

These additional data allowed for improved resolution and imaging of potential geothermal features in the subsurface, down to a depth of 7km. The subsequent inversion of these data, together with all other collected data has revealed new prospectivity in addition to the prospectivity already identified from the 2023 survey data (Figure ii). Three (3) shallow targets have been identified beneath well imaged clay caps (targets 1, 2 and 3 on Figure ii) in addition to a deeper target (target 4 on Figure ii) associated with a probable partial melt zone. The large and deep low resistivity geobody shown in Figure ii is likely to represent a series of magma storage chambers and vertical dykes, lying obliquely beneath the central cone of Augustine volcano at a depth of between 2km and 6km below sea-level. Data from the Alaska Volcano Observatory (AVO) suggest temperatures within this magma zone could exceed 840°C. With these new findings, a better analogue for Augustine is the Kakkonda Field, NE Honshu, Japan which currently produces in excess of 60Mwe from shallow and deep reservoirs.

New and refined volumetric and economics Montecarlo simulations indicate an overall P50 of 204MWe with a P10-P90 range of 167-243Mwe. Table I summarizes our key parameters and assumptions, while Table II summarizes the new P50 case economics.

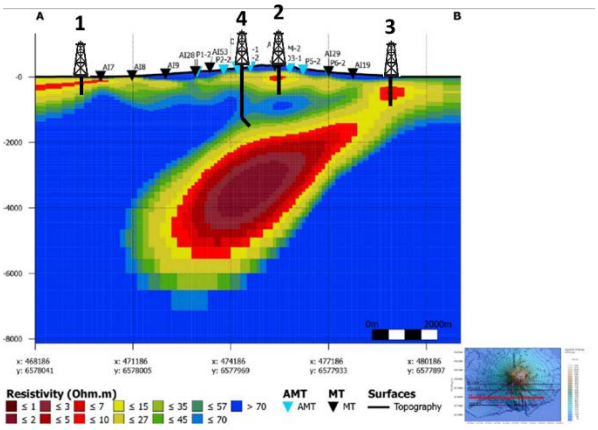

Figure ii. MT resistivity cross section across southern Augustine Island

Prospect	P50 (MWe)	P90-P10 (MWe)	Most likely temp (°C)	Estimated area (km²)	Estimated reservoir thickness (m)
1 (SW)	44	23-65	150	6.5	400
2 (Central)	65	47-83	275	4.3	400
3 (SE)	21	15-26	225	1.7	400
4 (Deep)	74	47-101	450	5	150
Overall	**204**	**167-243**			

Table I. New volumetrics, key parameters & assumptions

P50 case	
	CAPEX/MW: $2.5M
	IRR (35 years): 34%
	NPV (35 years): $977M
	Pay out: 10 years from start-up

Table II. New economics, key numbers, P50 case

GeoAlaska

Mission

GeoAlaska's mission is to deliver sustainable, affordable, carbon-neutral, baseload geothermal energy to the benefit of Alaska's residents and the State's economic future.

By fulfilling this mission, GeoAlaska will ensure long-term energy security for Alaska. Through innovation, strategic partnerships, and a commitment to environmental stewardship, GeoAlaska aims to energize Alaska's future by developing Alaska's vast geothermal potential.

Vision

GeoAlaska's vision is to be an industry leader in geothermal energy, transforming Alaska into a model of sustainable energy independence. By tapping into the State's vast geothermal resources, we envision a future where Alaska's economy thrives on clean, reliable, baseload geothermal power.

About

Founded in May 2020, GeoAlaska is committed to addressing Alaska's energy needs by harnessing the geothermal potential within the Cook Inlet basin, focusing on Mt. Spurr and Augustine Island. GeoAlaska's plan is to provide carbon-neutral, long-term energy security for the Alaska Railbelt grid, which serves 65% of the state's population.

Our journey began by securing a State of Alaska geothermal permit on Mount Spurr in September 2021, followed by a permit on Augustine Island in September 2022. GeoAlaska partnered with Ignis Energy – an international leader in the geothermal industry - during March 2023, and then expanded our presence on Augustine Island by securing another geothermal permit during April 2024.

Homer Electric Association (HEA) and GeoAlaska entered into a strategic agreement during 2022. On the heels of this agreement, HEA was funded by the Alaska Energy Authority (AEA) to study the feasibility of connecting power produced at Augustine Island to the grid through a 70-mile subsea HVDC transmission line. GeoAlaska actively cooperates with the Alaska Volcano Observatory (AVO) to advance the AVO's research and volcano monitoring mission.

GeoAlaska and our strategic partners are focused on building a better future through the development of sustainable, baseload geothermal energy to the benefit of all Alaskans.

www.geoalaska.com

Vision

At Ignis H2 Energy, we are committed to driving a cleaner, sustainable future by developing affordable, reliable, and renewable geothermal energy as a stable baseload power source.

- Clean Energy: We aim to deliver sustainable geothermal energy that supports long-term environmental goals while providing dependable and cost-effective power.
- Unmatched Expertise: Drawing on our extensive experience in the Oil & Gas sector, we enhance every phase of geothermal development, from exploration to production.
- Balanced Portfolio: We collaborate with top industry leaders, proven technologies, and innovative solutions to build a diversified, reliable, and risk-managed project portfolio.

Mission

Ignis H2 Energy is advancing a portfolio of one gigawatt of proven geothermal reserves globally by 2030. Our robust opportunity review process ensures a risk-balanced portfolio that is:

- Geographically diverse
- Geologically diverse
- Geopolitically diverse

Our current portfolio includes key projects in:

- Türkiye: Kaynarpınar, Kargapazarı, Kantarkaya, Ilıpınar, Güzelkent
- USA: Mount Augustine, Mount Spurr, Nevada Basalt, Clear Lake Volcanic Field
- Italy: Isola di Vulcano

Additionally, we are actively reviewing opportunities in Germany, Indonesia, Utah, and New Mexico, further expanding our global reach.

About

Unlike other start-ups in the geothermal industry, Ignis H2 Energy does not focus on a single technology or opportunity but rather manages a risk balanced portfolio of different power producing opportunities around the globe in high enthalpy environments. This provides a broader diversification while applying proven technology and allowing shared learnings from our esteemed panel of geothermal experts across the portfolio. Ignis H2 Energy, founded in 2021, benefits from an existing support structure in most countries through its sister company Geolog International.

www.ignisenergy.com